PROCESS INTEGRATION OF

A GAS TO LIQUID PLANT AND A POWER PLANT

A Thesis

by

DONGHAK KIM

Submitted to the Office of Graduate and Professional Studies of
Texas A&M University
in partial fulfillment of the requirements for the degree of

MASTERS OF SCIENCE

Chair of Committee,	Mahmoud El-Halwagi
Committee Members,	M. Sam Mannan
	Waruna Kulatilaka
Interdisciplinary Program Chair,	Efstratios N. Pistikopoulos

August 2018

Major Subject: Energy

ABSTRACT

The gas-to-liquid (GTL) industry is vulnerable to the variation of the oil and gas market price. This shortcoming has forced future GTL projects to be suspended and even cancelled. As one of the measures to overcome the challenge the GTL industry faces, process integration of a GTL plant and a power plant via a F-T tail gas supply line is proposed.

The process integration allows an integrated plant to adjust F-T tail gas distribution that affects the production rates of two products, oil and electricity. The first result shows that recycling F-T tail gas to the GTL plant is superior to supplying tail gas to the power plant in the perspectives of power generation and utility consumption. However, recycling all F-T tail gas to the GTL plant is not feasible due to the constraints that both plants require. One constraint is the requirement to reduce nitrogen compound build up in F-T tail gas, whereas the other constraint is the limitation of modified wobbe index range from gas turbine fuel specification. Since the latter constraint covers the former constraint, the modified wobbe index limitation governs the allowable range of F-T tail gas fraction.

Despite the constraints, the integrated plant still has the flexibility on the adjustment of tail gas distribution. Within the feasible region, the integrated plant can be designed and operated by balancing multiple parameters including power generation, utility consumption and nitrogen compound buildup that have a trade-off relationship.

ACKNOWLEDGEMENTS

I would like to thank people for full supports on preparing my thesis. Above all, I really appreciate the guidance of Mahmoud El-Halwagi, my advisor, of the Department of Chemical Engineering. Without his guidance, I would not start and finalize my study. I will never forget his willingness to help my research.

I want to extend my gratitude to my Advisory Committee, Dr. Mannan and Dr. Kulatilaka, for their advice. I further have to thank Dr. Hilaly, the substitute of Dr.Mannan for my defense, Jinyoung Choi and Changwoo Lee for their support.

I would like to sincerely appreciate for the director of Energy Institute, Professor Efstratios Pistikopoulos, the academic program coordinator, Dr. Valentini Pappa, and the administrative staffs of the Energy Institute for their assistance and support during energy master's program.

Thanks also go to my friends and colleagues and the department faculty and staff for making my time at Texas A&M University a great experience. Finally, thanks to my mother and father for their encouragement.

CONTRIBUTORS AND FUNDING SOURCES

Contributors

This study was conducted under the guidance of my research advisor, Professor Mahmoud El-Halwagi, advisory committee members, Professor Sam Mannan of the Artie McFerrin Department of Chemical Engineering and Professor Waruna Kulatilaka of the Department of Mechanical Engineering. As the substitute of Professor Sam Mannan, Professor Ahmad Hilaly attended my defense for master's thesis.

All work for the thesis was carried out independently by the student.

Funding Sources

My graduate study is supported by a scholarship from Engineering Development Research Center in South Korea.

NOMENCLATURE

ATR	Auto Thermal Reforming
DLN	Dry Low NOx
DR	Dry Reforming
F-T	Fischer-Tropsch
GTL	Gas to Liquid
HTFT	High temperature Fischer-Tropsch
LHV	Lower Heating Value
LTFT	Low temperature Fischer-Tropsch
MNQC	Multi-Nozzle Quiet Combustor
MWI	Modified Wobbe Index
POX	Partial Oxidation
PSA	Pressure Swing Adsorption
SCR	Selective Catalytic Reduction
SMR	Steam Methane Reforming
TG	Tail Gas

TABLE OF CONTENTS

Page

LIST OF FIGURES

Page

LIST OF TABLES

Page

1. INTRODUCTION

A gas-to-liquid (GTL) process is one of the processes to monetize natural gas.[1] With the attention of the process, the number of GTL projects has increased throughout the years.[2] Also, it is expected that the GTL process will contribute to increase total liquid supplies by 2040.[3]

However, recently the recession of the GTL industry occurred. For instance, Shell cancelled a 140,000 bbl/day GTL project in 2013.[4] Sasol decided not to develop a $15 billion GTL project in 2017.[5] Both imply that the profit of a future GTL project is not guaranteed due to the uncertainties of oil and gas market prices and the variability of the gap between the prices.[6] While the GTL process has been improved in the perspective of water and energy sustainability,[1,7] it is not likely to break through the challenge the GTL industry has faced. In addition to improving process efficiency internally, a way to decrease dependence on oil and gas market conditions is needed. In this regard, an integrated plant that consists of a GTL plant and a power plant is proposed to alleviate the risk that exists under volatile oil and gas market prices.

The objective of this study is to evaluate the flexibility and feasibility of the integrated plant. A simulation model in ASPEN Plus is developed to reflect a process design modification and visualize the process of the integrated plant. The model helps to analyze the performance of the integrated plant with the adjustment of F-T tail gas distribution. With the simulation results, constraints that limit the split control range of F-T tail gas are included to find out feasible solutions.

2. PROCESS BACKGROUND

This study requires the understanding of the GTL plant, the power plant and the connection between the two. In particular, there are two ways to utilize the F-T tail gas generated by the Fischer-Tropsch synthesis. One way is that it is recycled to a syngas production unit in the GTL plant to enhance the productivity of GTL products, and the other way is that it is sent to a gas turbine in the power plant to generate electricity. Before the process configuration of the integrated plant is described, background information with respect to the GTL process, F-T tail gas utilization and the power generation process is given as below.

2.1 Syngas production process

A syngas production process is one of the most important processes in the GTL plant. The cost of a syngas production unit accounts for around 40% of total cost of the GTL plant.[7] Furthermore, downstream processes for GTL products are affected by syngas compositions. The syngas compositions need to maintain a desired ratio between hydrogen and carbon monoxide of 2:1 that a F-T reactor requires.[8] These aspects emphasize the selection of the syngas production process.

There are various kinds of ways to produce the syngas: steam methane reforming (SMR), partial oxidation reforming (POX), and dry reforming (DR).[9] Combined technologies such as auto-thermal reforming (ATR) and tri-reforming are also in development.[10] The combined technologies as well as SMR, POX and DR are involved with basic reactions.[11]

Steam methane reforming reaction

$CH_4 + H_2O \rightarrow CO + 3H_2$ $\Delta H_{298} = 206$ kJ/mol

Partial oxidation reforming reaction

$CH_4 + \frac{1}{2} O_2 \rightarrow CO + 2H_2$ $\Delta H_{298} = -36$ kJ/mol

Dry reforming reaction

$CH_4 + CO_2 \leftrightarrow 2CO + 2H_2$ $\Delta H_{298} = 247$ kJ/mol

Water-gas shift reaction

$CO + H_2O \leftrightarrow CO_2 + 2H_2$ $\Delta H_{298} = -41$ kJ/mol

To begin with, the steam methane reforming is one of the most prevalent processes in the chemical industry in that it provides around 50% of total production of hydrogen.[12] The syngas that has a ratio between hydrogen and carbon monoxide of 3:1 is obtained through the steam methane reforming with catalysts.[13] In addition to the steam methane reforming reaction, the water-gas shift reaction helps adjusting the hydrogen content in the syngas.[14] However, the SMR reaction is an endothermic reaction that absorbs external energy to keep reactor temperature constant, which indicates that additional fuel and relevant equipment to provide heat energy are required. To overcome this disadvantage, an alternative method to supply the heat from the flue gas of another process has been proposed.[15]

When it comes to partial oxidation reforming, it produces syngas that consists of hydrogen and carbon monoxide of 2:1.[16] Compared to SMR, POX is not suitable to generate syngas that has a high concentration of hydrogen. However, it is a recommended ratio for Fischer-Tropsch (F-T) synthesis.[17] Moreover, an external heat source is not necessary because the POX reforming reaction is exothermic.

On the other hand, POX reforming demands pure oxygen provided from an air separation unit.[18] In terms of catalyst usage, the POX reforming reaction can occur regardless of the usage of catalysts.[16] However, the absence of the catalysts raises concerns about the formation of soot and nitrogen compounds such as ammonia and hydrogen cyanide (HCN), which are harmful to cobalt catalysts for F-T synthesis.[19, 20]

Dry reforming produces syngas that has a hydrogen and carbon monoxide ratio of 1:1. Despite the lowest ratio among three basic reactions, it is useful when combined with SMR to meet the requirement of H_2:CO ratio for F-T synthesis.[21] Moreover, the usage of carbon dioxide for syngas production can contribute to reduce carbon emission.[22] For example, carbon dioxide in flue gas leaving a power plant serves as a reactant for syngas production.[23]

Auto thermal reforming (ATR) is composed of SMR and POX. This reforming method uses oxygen and steam to generate syngas. Since the operating temperature for ATR is relatively low compared to that for POX reforming, ATR mitigates the formation of soot and nitrogen compounds.[19] Moreover, the amount of fuel for heating decreases, which is attributed to a combination of the endothermic reaction and the exothermic reaction.[24]

Tri-reforming is involved with all reforming reactions. This technology has three methods for syngas production, which are useful to adjust the H_2:CO ratio for F-T synthesis.[10] The various kinds of tri-reforming process configurations are developed including KOGAS tri-reformer.

In the view of energy utilization, combined processes such as ATR and tri-reforming process are more favorable than single reaction processes. Thermal efficiencies of the combined processes are likely to be 1 – 2 % higher than those of single reaction processes.[19] On the other hand, the processes associated with ATR or tri-reforming are so complex that it should be considered to balance the supplying of each source.

2.2 Syngas conditioning for CO_2 removal

The syngas generated by different types of reforming comprises carbon dioxide as well as main compositions, hydrogen and carbon monoxide. The carbon dioxide is not negligible because around 20 % of carbon in feed natural gas forms carbon dioxide.[25] Moreover, carbon dioxide is not likely to participate in F-T synthesis through water-gas shift activity if cobalt catalysts are applied.[18,20,26] Even the presence of CO_2 reduces the selectivity of heavy hydrocarbons on F-T synthesis.[27] For these reasons, the carbon dioxide in the syngas should be removed in advance of a F-T synthesis process if F-T tail gas is recycled to the syngas production process.[19]

2.3 Fischer-Tropsch synthesis

For the purpose of converting syngas to hydrocarbon chains, Fischer-Tropsch (F-T) synthesis is used. The representative formula of F-T synthesis is described as follows.[6]

$CO + 2H_2 \rightarrow (\text{-}CH_2\text{-})_n + H_2O$ (highly exothermic)

The hydrocarbons that have a wide range of carbon numbers are created though this synthesis. The formation of hydrocarbon chain growth is expressed by Equation 1), Anderson–Schulz–Flory (ASF) distribution equation.[28]

$x_i = (1 - \alpha) \times \alpha^{i-1}$……Equation 1)

The term α is the possibility of hydrocarbon chain growth, which governs hydrocarbon distribution according to carbon number i. When one alpha value does not represent all

hydrocarbon formulation, two alpha values are introduced to describe different chain probabilities.[28, 29]

F-T synthesis is divided into two categories by operating temperature of a F-T reactor. The difference between two categories are presented in Table 1.[6, 25, 27, 29]

Type	HTFT	LTFT
Operating temperature	300 - 350 ℃	220 – 240 ℃
Operating pressure	Around 25 bar	20 – 25 bar
Conversion rate	Above 85 %	Around 60%
Alpha value	0.65 – 0.7	0.85 – 0.95
Main products	Gasoline and low molecular mass olefins	High molecular mass waxes (synthetic fraction of diesel)
Catalyst	Fe	Co (or Fe)
Temperature control	Steam is supplied as a coolant to maintain operating temperature during exothermic F-T synthesis reaction.	

Table 1 The comparison of HTFT and LTFT

2.4 Syncrude upgrading

The syncrude generated from the F-T synthesis process goes into the syncrude upgrading process. This process converts the syncrude to various GTL products such as naphtha, gasoline, diesel, kerosene and other desired products through hydrocracking and fractionation.[1, 18] However, in this study the GTL products are not separated, and they are represented by one constant value. Also, the process is simplified by applying an assumption based on normal distribution probability for C_{20} or heavier hydrocarbons' cracking.[1] Since the separation of GTL products is not the focus

of this study, the simulation model for the syncrude upgrading process is developed in a uncomplicated manner.

2.5 F-T tail gas utilization and nitrogen compound buildup

The main purpose of F-T synthesis is to produce heavier hydrocarbons. However, F-T synthesis also generates residual gases including methane, hydrogen, carbon monoxide and nitrogen. The mixture of residual gases is defined as F-T tail gas.

The F-T tail gas can be discharged or utilized. It is simple to discharge the F-T tail gas to the atmosphere because it is not associated with any process. However, the disposal is not an adequate approach in terms of energy and environment sustainability. In addition to the disposal route, there are alternative routes for utilization presented in Figure 1.[29]

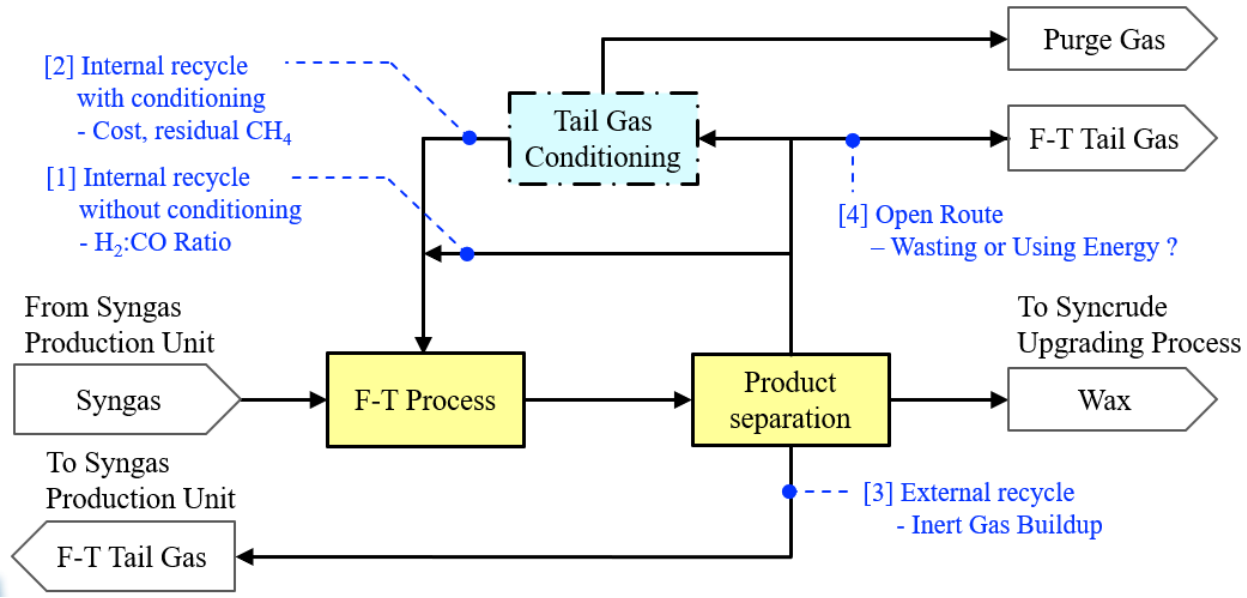

Figure 1 F-T tail gas utilization loops

The first alternative route is the internal recycling loop without conditioning through which the F-T tail gas is recycled to the F-T process. It improves the productivity of the F-T process because the F-T tail gas still contains hydrogen and carbon monoxide that are conducive to F-T synthesis. However, this route has an issue with adjusting the ratio of hydrogen and carbon monoxide. The ratio is not identical with the desired ratio for the F-T process. Furthermore, compared to iron catalysts, cobalt catalysts for the F-T process are not likely to encourage a water-gas shift reaction that can adjust the ratio.[26]

The second alternative route can resolve the issue on syngas constituents. The route includes the tail gas conditioning unit to meet the ratio for the F-T process. However, it has other problems such as high cost and residual methane. Installing the tail gas conditioning unit increases the total cost of a GTL process. Moreover, the residual methane still remains although the F-T tail gas passes through the tail gas conditioning unit.

The third alternative route resolves these problems. Since the route is connected to the syngas production unit, the desired ratio between hydrogen and carbon monoxide for F-T synthesis is achieved regardless of tail gas compositions. It does not need any additional conditioning unit. Furthermore, the residual methane mixed with natural gas can be converted to syngas via syngas reforming.[29] However, the route has an inherent disadvantage of recycling that F-T tail gas is not able to escape from a GTL process boundary. In particular, inert gases are confined in a GTL process. Carbon dioxide is separated by a carbon dioxide removal unit. Nitrogen, however, has no choice but to be accumulated in the GTL process.[29] Even a nitrogen separation unit is not preferable to the carbon dioxide removal unit because it is energy intensive and expensive.[30]

Although the nitrogen is unreactive, the buildup of nitrogen flow has an impact on the F-T process if partial pressure of carbon monoxide and hydrogen is changed.[31, 32, 33] In this regard, a

route for evacuating nitrogen is necessary to avoid establishing large nitrogen flow, rather than applying the F-T synthesis technology involved with nitrogen-rich syngas.[34] The paper that deals with this matter suggests to meet the 'soft maximum' specification of nitrogen flow as 15 %.[30] And lower nitrogen flow rate is preferred because nitrogen flow buildup increases the required capacity of equipment in the GTL plant.[30]

2.6 Heavy-duty gas turbine features

A gas turbine is one of the main equipment in a combined cycle power plant in addition to a heat recovery steam generator and a steam turbine. The gas turbine generates electricity and high temperature flue gas that allows the heat recovery steam generator to produce steam. In turn, the steam rotates the steam turbine to generate electricity. In this regard, a gas turbine has a vital role in generating electricity in a combined cycle power plant.

The gas turbine is capable of rapidly respond to variations in electricity demand. In the condition of peak load and cyclic load of electricity, the gas turbine can follow this load change and supply required electricity. This ability is expected to be more significant because it can offset the fluctuate power generated from renewable energy resources.[35]

While the gas turbine becomes prevalent in the power industry due to these advantages, it has the issue of fuel-flexibility. The fuel of the gas turbine is typically natural gas of which the main content is methane. However, fuel constituents are diversified, which requires fuel-flexible design on the gas turbine to expand its application. The design modification of a gas turbine combustor is inevitable to utilize low calorific fuel with flame stability.[36, 37, 38] When it comes to gas turbine material, the materials of major components of the gas turbine need to be improved for syngas firing.[39]

In addition to the gas turbine material, the fuel flexibility is related to the type of a gas turbine combustor. For instance, the applications of Dry Low NOx (DLN) combustors with fuel-air premixing are restricted due to the risk of flashback around the burner.[37] The DLN combustors can cover up to 48% of hydrogen content fuels with holding flame.[40] On the other hand, a Multi-Nozzle Quiet Combustor (MNQC), one of the diffusion type combustors, has the capability to cover a wider range of syngas fuel that contains a hydrogen content up to 90%.[41] Moreover, the MNQC H_2 testing is conducted with fuels that have low heating values and high hydrogen concentrations. With the advancements of gas turbine technology, gas turbine manufacturers have gained operating experience on the projects where fuel-flexible gas turbines are installed. [42]

2.7 Selection of power plant configuration

The gas turbine features described in Section 2.6 support that a combined cycle power plant is an appropriate configuration for process integration. The fuel-flexible gas turbine can accept the fuel mixture containing hydrogen, carbon monoxide, methane and other compositions.[41, 43] Moreover, the power plant with the gas turbine outweighs that with a boiler in terms of efficiency and specific price (tariff). Several power plants are evaluated based on capacity, specific price and net efficiency in Table 2.[44]

Type of plant	Capacity	Specific price (US$/kW)	Net efficiency (%) - LHV basis
Combined cycle power plant	800 MW	550 – 650	55 – 59
Combined cycle power plant	60 MW	700 – 800	50 – 54
Gas turbine plant (simple cycle)	250 MW	300 – 400	38 – 40
Gas turbine plant (simple cycle)	60 MW	500 – 600	35 – 42
Steam power plant (coal)	800 MW	1200 – 1400	(42 –) 47
Steam power plant (coal)	60 MW	1000 – 1200	30 – 35

Table 2 The comparison of power plants by capacity, specific price and efficiency

Since a power plant is supposed to be operated continuously for supplying auxiliary power of a GTL plant as well as making a profit, the net efficiency is the highest priority among the key specifications described in Table 2. Therefore, a combined cycle power plant is superior to a simple cycle power plant or a steam power plant for process integration.[44]

3. PROBLEM STATEMENT

In this study, process integration of a GTL plant and a power plant is investigated. Process integration establishes an alternative configuration to produce oil and power. It provides an initial result after simulation and modeling. The result, however, is involved with constraints that are derived from the limitation of each plant design and operation. The constraints revise the initial result and eventually give feasible solutions. On the progress of this process integration, there are key issues to consider as follows:

- What are features of an alternative configuration?
- What is the result of process integration in the perspectives of power output and utility consumption?
- Are there any constraints that prevent a simulation model from being feasible?
- How is the allowable range of F-T tail gas fraction with constraints?
- What is the difference between an initial result and a revised result?

4. METHODOLOGY

Process integration takes several steps to develop an integrated plant model. To begin with, a base configuration and an alternative configuration are both defined. The base configuration consists of two individual plants, the GTL plant and the combined cycle power plant, that are not combined with each other. This configuration is illustrated in Figure 2.

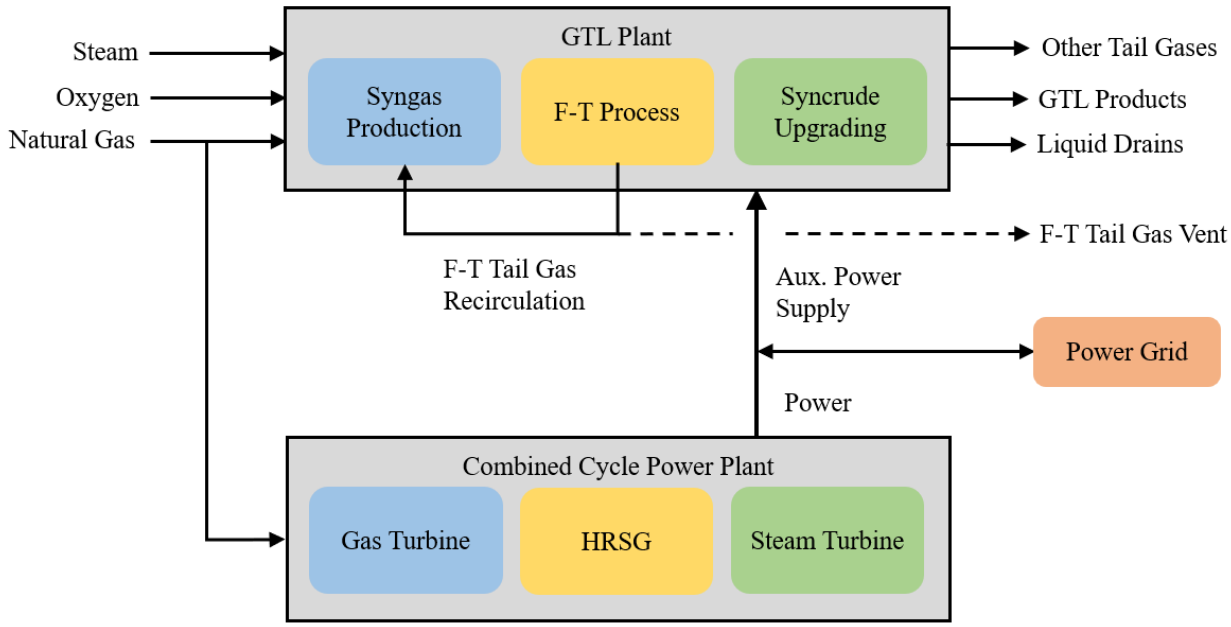

Figure 2 Base configuration of the GTL plant and the combined cycle power plant

The only aspect that both plants have in common is to use natural gas as a source. The GTL plant converts natural gas to GTL products such as naphtha, gasoline, diesel, kerosene and others, whereas the combined cycle power plant consumes natural gas to generate electricity. This aspect gives a benefit that both plants are accessible to a natural gas pipeline. The other benefit that the base configuration has is power sustainability. Auxiliary power of the GTL plant can be supplied from the power plant, which allows the GTL plant to be a self-sufficient plant with regard to

electricity. In the GTL plant, the F-T tail gas from the F-T process is recycled to the syngas production unit to increase GTL products' rate. Otherwise, the tail gas is emitted to the atmosphere. Other tail gases and liquid drains are discharged.

On the other hand, an alternative configuration is composed of two interconnected plants through the F-T tail gas supply line. Figure 3 shows the configuration.

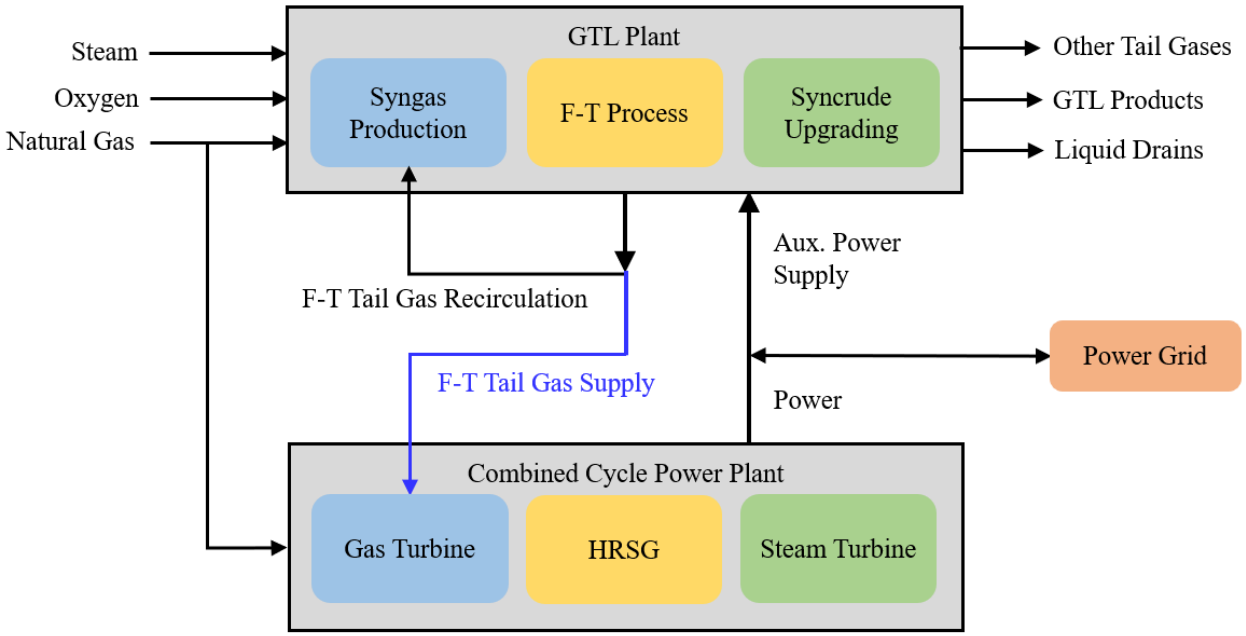

Figure 3 Alternative configuration of an integrated plant

The main difference between both configurations is the methods of utilizing the F-T tail gas. In the base configuration, all the F-T tail gas goes back to the syngas production unit. The alternative configuration, however, has another route to supply the F-T tail gas to the gas turbine in the power plant. With this connection, the tail gas is utilized not only as a source for enhancing the productivity of the GTL plant but also as fuel for the power plant. The alternative configuration also has the advantages such as power sustainability and natural gas accessibility. On the contrary, the fuel gas treatment system in the power plant becomes complicated in that the tail gas as well

as natural gas is provided. Whether the power plant has the capability to cover fuel variation is important to establish the alternative configuration.

The next step is to create and develop a simulation model in ASPEN Plus. In the power engineering field, the programs such as GT Pro and Thermoflex are commonly used. However, they do not have functions to implement chemical reactions. Moreover, a limited number of fluid properties are available in the programs. Thus, the power plant process is created in ASPEN Plus flowsheet with the GTL process.

After the implementation of the simulation of an integrated plant, simulation results of two cases are evaluated. One case is to recycle all F-T tail gas to a GTL plant, whereas the other case is to supply all the F-T tail gas to a power plant. Power plant fuel is not blended together, and both cases are compared based on power output, steam consumption and oxygen consumption.

The former results are analyzed without any constraints and fuel blending. However, constraints need to be considered for the results to be more feasible. The constraints that limit process integration come from both the GTL process and the power plant process. On the GTL process, unnecessary nitrogen flow is built up in the main stream. This phenomenon is mitigated by adjusting F-T tail gas fraction that is the amount of F-T tail gas sent to a power plant. Identifying the allowable range of the F-T tail gas fraction defines the first constraint.

Adjusting the F-T tail gas fraction implies blending F-T tail gas and natural gas. The adjustment leads to the variation of fuel compositions, which in turn changes the Modified Wobbe Index (MWI) value. It should be within its permissible range that a gas turbine has. Complying with this requirement settles the second constraint.

Last, the simulation results are revised by two constraints from each plant. The performance of an integrated plant is assessed based on the revised results.

5. PROCESS DEVELOPMENT

The first step of process integration is to define the conditions at plant boundary. One of the conditions is natural gas compositions described in Table 3.[1, 45]

Component	Mol %
Methane	95.39
Ethane	3.91
Propane	0.03
Carbon Dioxide	0.59
Nitrogen	0.08
Temperature (°F)	79
Pressure (psia)	310

Table 3 Natural Gas Composition

The composition of natural gas supplied to the GTL plant is identical with that supplied to the power plant. The total flow rate of natural gas supplied to both plants is constant.

The other boundary condition is GTL production rate, which is assumed as 4,000 bbl/day.[6] The scale of simulation is smaller than that of recent projects.[18] However, actual GTL plants with similar capacity exist and are in operation.[46] Also, the capacity is appropriate for process integration with one gas turbine when considering the capacity. For these reasons, the small-scale GTL plant is developed in a flowsheet.

5.1 Syngas production process

The syngas production process in a GTL plant is based on tri-reforming, which requires three sources: steam, oxygen and carbon dioxide. High-pressure steam of which pressure and temperature are 435 psia and 79°F is necessary for steam methane reforming. Pure oxygen from an air separation unit is provided to the syngas production unit for partial oxidation reforming. Carbon dioxide gas is from a CO_2 removal unit located in between the syngas production process and the F-T synthesis process. Thus, there is no external CO_2 source. Its origins are natural gas and the product of tri-reforming reactions.

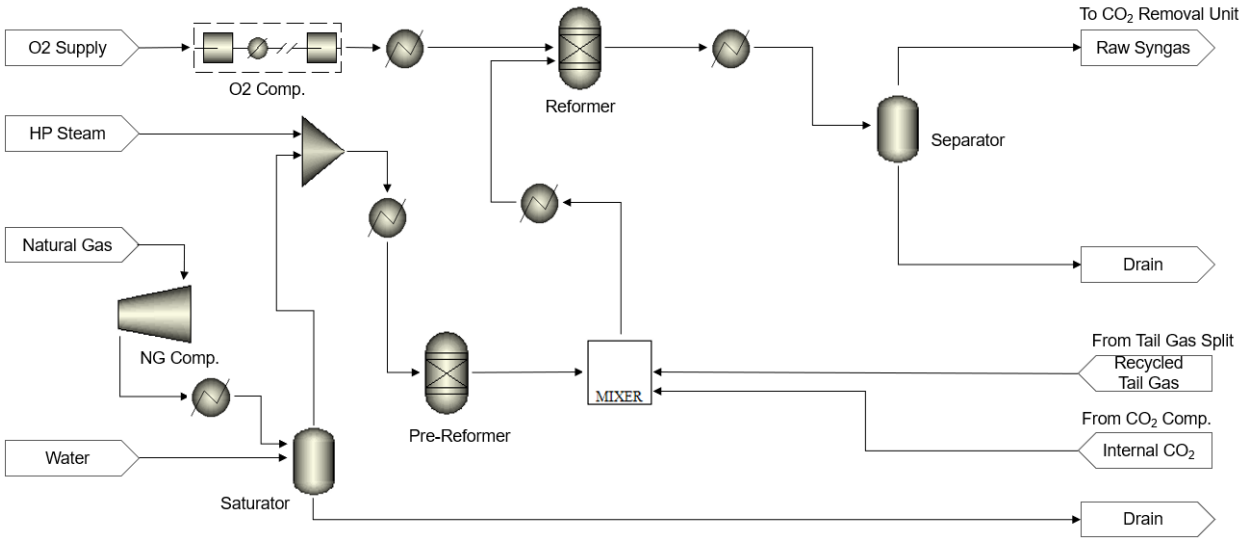

Figure 4 Syngas production process flow diagram[1]

The syngas production process starts with compressing natural gas. The natural gas is pressurized up to the operating pressure of reformer, 435 psia. Then it is heated by the heat exchanger to 300 °F and mixed with water on the saturator. In the saturator, heat energy that the natural gas contains vaporizes the water, and the natural gas temperature is decreased accordingly

due to latent heat of vaporization of water.[47] The saturated natural gas is combined with the high pressure steam before going to the pre-reformer. The pre-reformer plays a role in changing hydrocarbons except methane to hydrogen and carbon monoxide and preventing the coking phenomenon in the main reformer.[29] Ethane and propane constituents in the natural gas react with steam, which produces syngas. The exiting fluid from the pre-reformer is mixed with carbon dioxide and F-T tail gas. Then the mixture passes through the heat exchanger and the main reformer. The heat exchanger upstream of the reformer is required to keep the reformer in adiabatic condition. The reformer temperature is 1950 °F, which maintains constant by balancing an endothermic and exothermic reaction.[48] The oxygen gas supplied by the oxygen compressor reacts with methane, which generates syngas and heat. The steam that moves with the natural gas concurrently consumes the heat for the steam methane reforming reaction. The oxygen to carbon ratio is 0.6,[29] and the syngas from the reformer meets the ratio between hydrogen and carbon monoxide of 2.1 to 1.[49, 50] Since the temperature of the syngas from the reformer is high, it is cooled to 122 °F by the downstream heat exchanger and sent to the separator. In the separator, the syngas with CO_2 and residual methane is separated from condensed liquid. It goes into the CO_2 removal unit.

5.2 CO_2 removal and hydrogen separation process

In the CO_2 removal unit, CO_2 is removed from the syngas. The removal rate is set as 99.96%.[7] Most of the separated CO_2 is discharged to the atmosphere if the CO_2 gas is not used. However, the syngas production unit utilizes CO_2 for the dry reforming process. Thus, it is compressed by the CO_2 compressor to meet the operating pressure of the reformer and mixed with other gases.

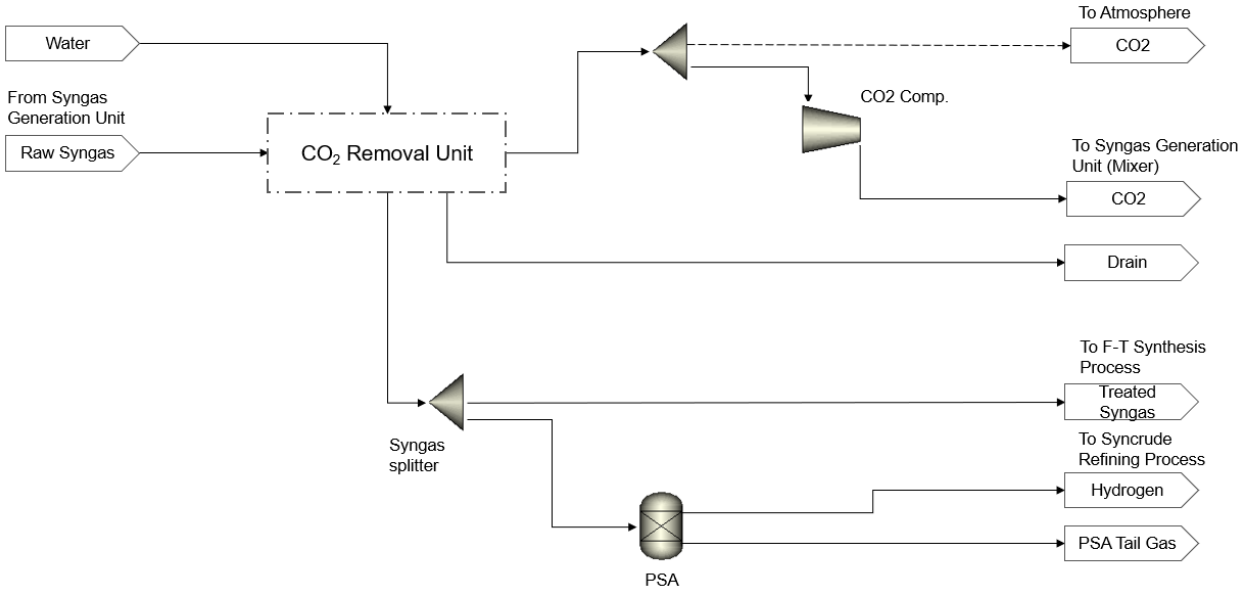

Figure 5 CO2 removal and hydrogen generation process flow diagram[1]

The syngas splitter divides the treated syngas into two branches as shown in Figure 5. One branch is connected to the F-T synthesis process, whereas the other branch is connected to the PSA unit. The amount of the treated syngas on the other branch depends on the hydrogen amount required for the syncrude upgrading process. The rest of the treated syngas is sent to the F-T synthesis process.

In the PSA unit, pure hydrogen is separated from other gases. The hydrogen is provided to the syncrude refining process for hydrogenation. Other gases are discharged to the atmosphere.

5.3 F-T Synthesis Process

The treated syngas from the CO_2 removal unit is fed to the F-T reactor. The operating pressure of the F-T reactor is 363 psia,[7] and the operating temperature of the F-T reactor and chain

growth probability (alpha value) are 428 °F and 0.92, respecitvely.[51, 52, 53, 54] Since the reaction that occurs in the F-T reactor is exothermic, the operating temperature can increase without any external heat. A cooling fluid prevents the increase in the operating temperature. In terms of F-T synthesis, the F-T reactor block implements the F-T synthesis reactions that produce only from C_1 to C_{30} hydrocarbons.[1]

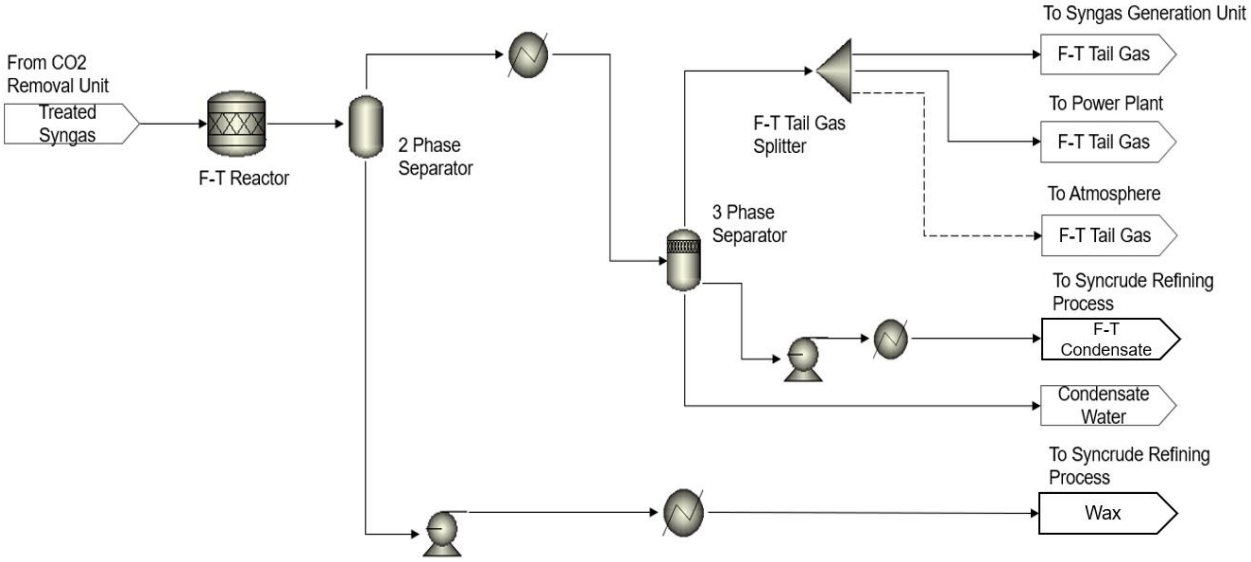

Figure 6 Fischer-Tropsch synthesis process flow diagram[1]

The separation of the F-T reaction products takes place through two steps. First, the 2-phase separator separates heavy hydrocarbons' liquid, which is called wax, from the products. Nonetheless, it still has heavy hydrocarbons to be supplied to the syncrude refining process. Before going to the 3-phase separator, its temperature is decreased by the downstream heat exchanger, which leads to the condensation of residual heavy hydrocarbons and water. The fluid fed to the 3-phase separator is divided into three fluids that are F-T tail gas, oil and water. The residual heavy hydrocarbons are pumped to the syncrude refining process while the water is drained. The F-T tail

gas leaving the separator can be supplied to the syngas production unit, a power plant or the atmosphere. The fraction values are controlled by the F-T tail gas splitter. In this study, the route to disposing the F-T tail gas to the atmosphere is disregarded. Instead, the F-T tail gas is sent through two other routes. The underlying reason is to maximize the utilization of the F-T tail gas.

In addition to the three routes described in Figure 6, There is a route through which the F-T tail gas is used as heating fuel for the GTL process. However, the route is excluded, which underlies the information that the minimum heat requirement is zero through heat integration.[1]

5.4 Syncrude upgrading process

The wax and F-T condensate from the F-T synthesis process are fed to the hydrocracker that serves to convert long hydrocarbon chains to short hydrocarbon chains. The short hydrocarbon chains react with the hydrogen supplied from the PSA unit, which primarily produces the mixture of desired hydrocarbons. As it leaves the hydrocracker, the mixture passes through the hot separator and the cold separator and coolers between the hydrocrackers and the cold separator.[54] Some gases vaporized on the cold separator are recycled to the hydrocracker with hydrogen, whereas other gases are emitted to the atmosphere.[1] The mixture from the cold separator is heated by the heat exchanger and enters the fractionator. Consequently, the final GTL products are obtained. In addition to the products, the light gas is vaporized and discharged to the atmosphere, while residual heavy hydrocarbons are recycled to the hydrocracker.[55]

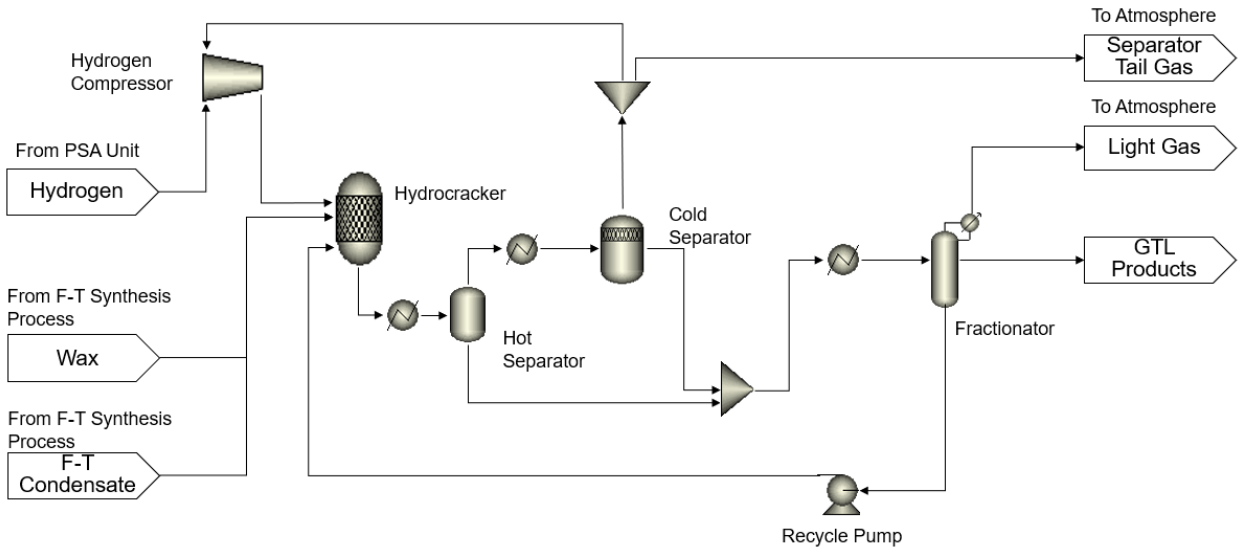

Figure 7 Syncrude upgrading process flow diagram[1]

5.5 Combined cycle power generation process

The other process integrated with the GTL process is the combined cycle power generation process illustrated in Figure 8. The process consists of three main equipment, the gas turbine, the heat recovery steam generator and the steam turbine, and relevant auxiliary equipment.

The gas turbine operates on the mixture of the natural gas and the F-T tail gas. The flow of each gas depends on the GTL plant operation. For example, the F-T tail gas flow for the power plant increases as the F-T tail gas flow for the GTL plant decreases. Since the decrease in the F-T tail gas recirculation to the GTL plant reduces the plant productivity, the GTL plant consumes more natural gas. In turn, the natural gas flow for the power plant decreases while keeping total flow of natural gas constant. In summary, in terms of power plant fuel, F-T tail gas flow increases as natural gas flow decreases, and vice versa.

Once two types of gases are blended, the blended fuel is heated by the performance heater up to 338 °F before combining with air. The air is compressed by the air compressor of which

pressure ratio on the design condition is 13.[56] The air compressor flow rate is controlled by the function to maintain the constant temperature, 2218 °F, at the gas turbine inlet. The isentropic efficiency and mechanical efficiency of the air compressor are 91.5 % and 99.6% at design point, respectively.[57]

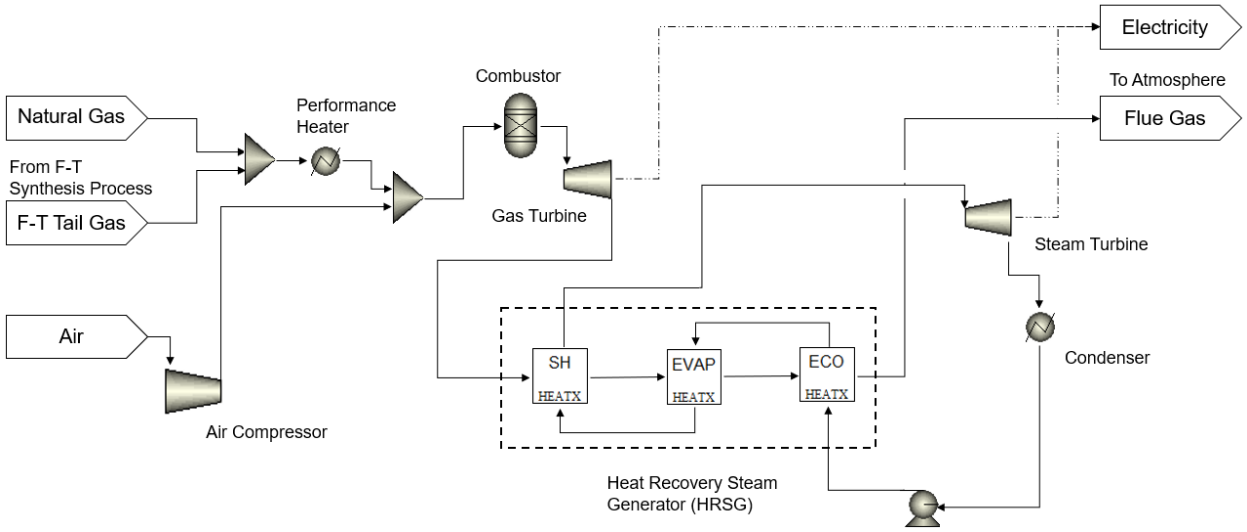

Figure 8 Combined cycle power generation process flow diagram[58]

The blended fuel and air are mixed and supplied to the combustor that is represented by RGibbs model in ASPEN Plus. The combustor changes the gas compositions and raises the gas temperature to provide heat energy to the gas turbine. On the other hand, the pressure in the combustor remains constant by ignoring the pressure loss across the combustor.

The combustion gas is sent to the gas turbine. The gas transfers heat energy to the gas turbine, which generates electricity. The input parameters of the gas turbine are presented in Table 4.

Parameters	Value	Remark
Isentropic Efficiency [59]	0.88	
Mechanical Efficiency	0.996	It is assumed as the same value from air compressor mechanical efficiency.
Outlet Pressure	1 atm	The pressure drop of subsequent equipment is ignored.

Table 4 Gas turbine input parameters

In addition to generating power, the gas turbine discharges exhaust flue gas that has less energy than the combustion gas. However, it still has sufficient heat for utilization. Before being discharged to the atmosphere, the flue gas provides heat to the heat recovery steam generator.

The heat recovery steam generator is composed of three components: the economizer, the evaporator and the superheater. For the single pressure HRSG, [60] each component is represented by one block in ASPEN Plus flowsheet. The key parameters regarding the components are described in Table 5.

Parameters	Value	Remarks
Superheated steam temperature	968 °F	Assumed
Superheated steam pressure	1450 psia	Assumed
Pinch point temperature difference	14.4 K	Assumed.
Water temperature at economizer inlet	91 °F	It is derived from the water temperature at the boiler feedwater pump outlet.

Table 5 Heat recovery steam generator input parameters

When it comes to the superheated steam temperature and pressure, they indicate the properties of the steam supplied to the steam turbine. The pressure is also associated with water saturation temperature on the evaporator. The water saturation temperature is one of the values for calculating pinch point temperature difference. The definition of pinch point temperature difference is the gap between the water saturation temperature and the temperature of flue gas leaving the evaporator, which is illustrated in Figure 9. In addition to the pinch point temperature difference, the water temperature at the economizer inlet is defined. These values determine the steam flow rate.

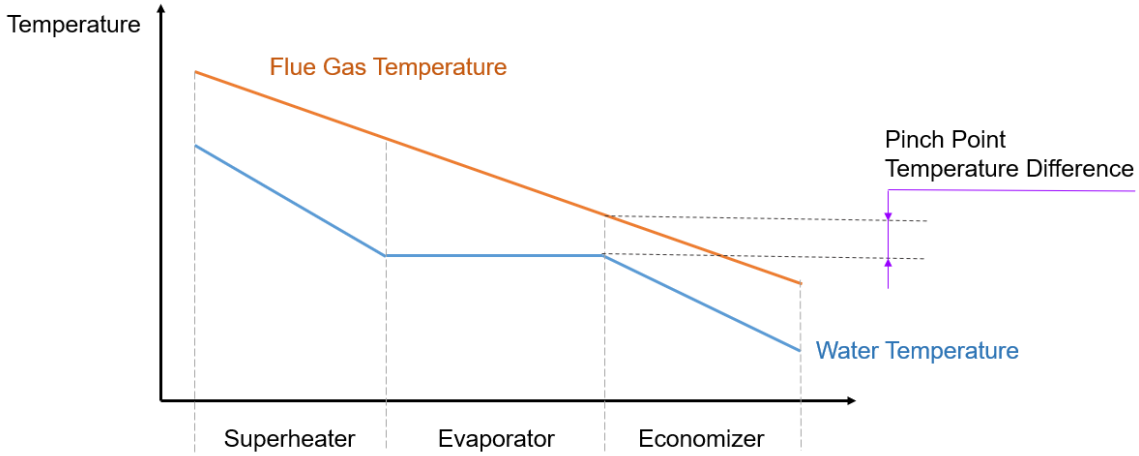

Figure 9 Pinch point temperature in HRSG [61]

The steam exiting the heat recovery steam generator goes to the steam turbine. The steam turbine is the other equipment that generates electricity with the gas turbine. The input parameters for the steam turbine is specified in Table 6.

Parameters	Value
Steam turbine exhaust pressure [59]	0.696 psia
Steam turbine isentropic efficiency [62]	0.8098
Steam turbine mechanical efficiency [63]	0.9532

Table 6 Steam turbine input parameters

The steam turbine exhaust pressure is identical with downstream condenser pressure. The latent heat of steam is removed on the condenser where the exhaust steam is condensed. The subcooled temperature of the condenser is set as 1 ˚F, which is referred from HEI Surface Condenser Standard. The water stored in the condenser is pumped by the boiler feedwater pump. By supplying the water to the heat recovery steam generator, a power plant cycle is set up in ASPEN Plus flowsheet.

5.6 The consideration of an off-design condition for a combined cycle power plant

The established power plant cycle is based on the design condition. The key parameters in the flowsheet are appropriate to investigate the combined cycle power plant at one specific condition. However, they do not cover off-design conditions in which fuel composition and flow rate varies. The simulation model needs to be equipped with additional functions that modify the parameters for off-design conditions.

As described in Section 5.5, the mixture of natural gas and F-T tail gas varies in its composition and flow rate, which results in a change in heat input to the power plant. A design condition is defined as the state that the heat input is the highest value. Conversely, off-design

conditions correspond to all other states in which the heat input is below maximum. Based on these definitions, the sequence of changes in the key parameters is described in Figure 10.

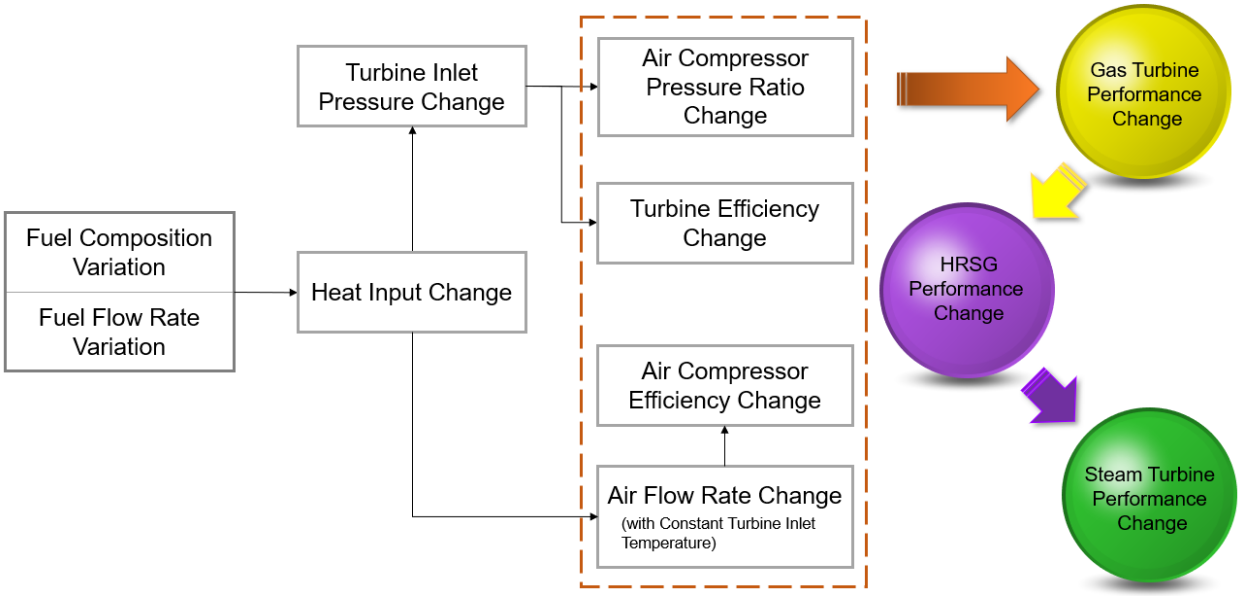

Figure 10 The relationship diagram of fuel variation and power plant performance

Figure 10 shows how the major parameters of the power plant are changed sequentially. To begin with, the change in heat input affects two parameters: air flow rate and turbine inlet pressure. The air flow rate is manipulated in order to maintain a constant temperature. When the heat input decreases, turbine inlet temperature will decrease. However, the temperature is not changed by reducing the air flow rate. The function that keeps the temperature constant is included in the simulation model, which is described in Figure 11.

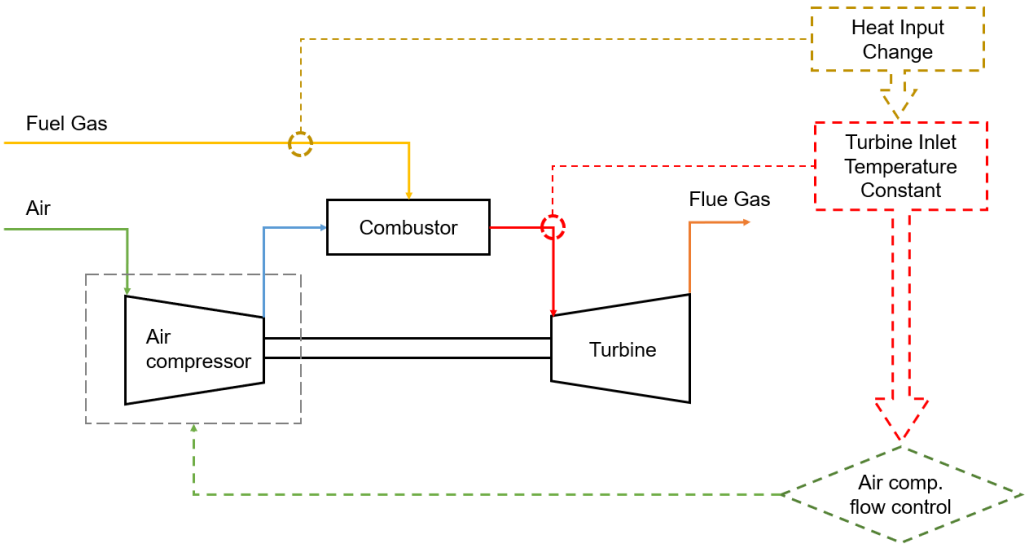

Figure 11 Air compressor flow control scheme

The change in the air flow rate influences air compressor's isentropic efficiency. Since the air compressor is designed to have the highest efficiency at the design point, the efficiency in an off-design condition is lower than that in the design condition. The efficiency of the air compressor is expressed by Equation 2) and Equation 3).[64]

$$\eta_{comp} = \eta_{comp,d} \times \frac{0.3337 + 1.0917 \times M_r - 0.5254 \times Mr^2}{0.9} \quad \text{Equation 2)}$$

$$Mr = \frac{\dot{m}_{comp}}{\dot{m}_{comp,d}} \quad \text{Equation 3)}$$

The efficiency (η_{comp}) is the function of air mass flow ratio (Mr), and the air mass flow ratio is obtained by an air flow rate divided by the air flow rate in the design condition. The air mass flow ratio is 1 or less because the design condition has the largest air capacity that is required for keeping the turbine inlet temperature constant with the highest heat input.

In addition to the air flow rate, turbine inlet pressure is also dependent on fuel specification. The basic criteria for the turbine inlet pressure is to assume that choked flow is established at the first vane of a gas turbine.[65, 66] Based on this assumption, the equation describing a choked flow can be introduced for turbine inlet pressure calculation. It is shown as Equation 4). [65, 67]

$$\dot{m} = p_o \times A \times \sqrt{\frac{\gamma \times M}{Z \times R_u \times T_0} \left(\frac{2}{\gamma+1}\right)^{\frac{\gamma+1}{\gamma-1}}} \quad \text{Equation 4)}$$

$$\frac{\dot{m}}{P} \times \sqrt{\frac{T_o}{M}} = (constant) \quad \text{Equation 5)}$$

Equation 5) is the formula derived from Equation 4). The compressibility factor (Z) and the heat capacity ratio (γ) are regarded as unchanged values.[67] The nozzle area (A) that combustion gas passes through remains constant because the gas turbine is not physically modified during its operation. The universal gas constant (R_u) is also a constant value. These things considered, Equation 5) is obtained as a simplified formula that contains the mass flow ($\dot{m}$), the molecular weight (M), the turbine inlet temperature (T_o) and the pressure (P) at the turbine inlet point.[36, 68] Since turbine inlet temperature is constant in the simulation model,[69] the turbine inlet pressure is the function of the mass flow and the molecular weight.

Turbine inlet pressure has influence on other key parameters, namely air compressor pressure ratio and turbine isentropic efficiency. The air compressor pressure ratio should be consistent with the turbine inlet pressure in order to supply required air flow rate for combustion. The fuel supply pressure should also not be less than the turbine inlet temperature. Both the air compressor pressure ratio and the fuel supply pressure are modified as turbine inlet pressure changes.

In addition to air compressor pressure ratio, turbine isentropic efficiency relies on the turbine inlet pressure. The equation that represents this relationship is described as Equation 6).[64]

$$\eta_{\text{turb}} = \eta_{turb,\text{d}} \times \frac{0.6164+0.6179 \times P_r - 0.3343 \times Pr^2}{0.9} \quad \text{Equation 6)}$$

$$\text{Pr} = \frac{P_{turb}}{P_{turb,d}} \quad \text{Equation 7)}$$

To calculate the turbine isentropic efficiency (η_{turb}), the turbine inlet pressure ratio (P_r) at between the design condition and an off-design condition is presented in Equation 7). In the design condition, the turbine inlet pressure comes from the pressure ratio of the air compressor.

In summary, a gas turbine specification in an off-design condition is different from that in the design condition. The revised values are aligned with not only a gas turbine but also a heat recovery steam generator and a steam turbine. The flue gas properties, such as flow rate and temperature, are changed by the revised values. The amount of heat absorbed by water (or steam) in the downstream heat recovery steam generator is changed, which results in the change in steam flow rate. In turn, the output of the steam turbine is changed.

6. CASE STUDY AND RESULT

6.1 The integrated plant performance based on different fuels without blending

The first investigation is the evaluation of the integrated plant performance according to fuel types for the power plant. As described in the section 4, the power plant receives either F-T tail gas or natural gas. Under the condition that the gases are not mixed, two cases are compared. Case I is to supply only the F-T tail gas to the power plant, whereas Case II is to supply only the natural gas to the power plant with setting up the F-T tail gas recycle loop through which all the F-T tail gas is recirculated to the GTL plant. The study result is summarized in Table 7.

Results	Case I	Case II	Remarks
Natural Gas (total, lb/hr)	93,249	93,249	
to GTL Plant (lb/hr)	58,738	93,246	
to Power Plant (lb/hr)	34,511	3	1) Natural gas flow rate conversion : 34,511 lb/hr = 2,057 lbmol/hr
Tail Gas (total, lb/hr)	63,746	55,726	
to GTL Plant (lb/hr)	63,746	0	1) Without nitrogen, the tail gas flow rate in Case I would be 56,709 lb/hr.
to Power Plant (lb/hr)	0	55,726	1) Tail gas flow rate conversion : 55,726 lb/hr = 4,932 lbmol/hr 2) Without nitrogen, the tail gas flow rate in Case II would be 55,602 lb/hr.
Steam Consumption (lb/hr)	58,026	79,999	
Oxygen Consumption (lb/hr)	73,520	108,921	
GT Fuel LHV (MMBtu/scf)	931	346	1) The values are referred to ASTM D3588-98.
Heat Input to Power Plant (MMBtu/hr) – LHV Basis	727	647	
Gross Power Output (MW)	118	106	
Auxiliary Power (MW)	16	22	
Net Power (MW)	102	84	

Table 7 Integrated plant performance (Case I and II)

Table 7 presents switching the power plant fuel from the natural gas to the F-T tail gas decreases net power output by 17%. The causes of this result are heat input to the power plant and auxiliary power consumption. In case of the heat input, it is the function of a fuel flow rate and a fuel LHV. The flow rate of the F-T tail gas is higher than that of the natural gas, whereas the natural gas LHV is higher than the F-T tail gas LHV. Between the flow rate and the LHV, the latter outweighs the former, which determines the heat input. In turn, the net power output has a higher value in Case I than Case II.

Auxiliary power consumption encourages the gap between each net power output to be larger. The major power consumers are the air separation unit and its downstream oxygen compressor. Since oxygen is consumed more in Case II than Case I, the power consumption of the air separation unit and the oxygen compressor is also higher in Case II than Case I. It is the other factor that cuts down on the net power output.

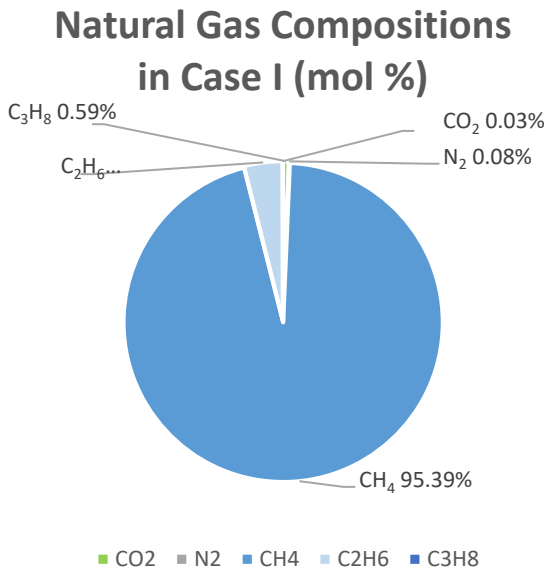

Figure 12 Natural gas constituents in Case I

In terms of the consumption of utilities including oxygen and steam, Case I is superior to Case II as well. In other words, both utilities are required more in Case II than in Case I. It results from the composition difference between the recycled F-T tail gas and the natural gas. The F-T tail gas shown in Figure 13 is a kind of syngas, the mixture primarily of hydrogen and carbon monoxide. The gases account for nearly 90% of total mole fraction. Compared to natural gas compositions illustrated in Figure 12, they are beneficial for the syngas production process because reforming reactions are not necessary. The only methane residual in the recycled tail gas reacts with oxygen or steam. On the other hand, Case II entails more oxygen and steam to generate the F-T tail gas supposed to go to the power plant.

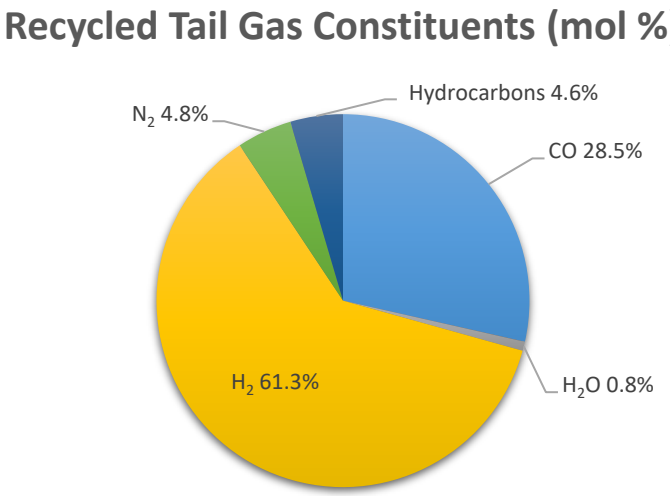

Figure 13 Recycled tail gas constituents in Case I

When it comes to tail gas flow rates in both cases, they are quite different. However, their gap decreases if nitrogen is disregarded from each flow rate. In particular, the tail gas flow rate in Case I is reduced from 63,746 lb/hr to 56,709 lb/hr, which is similar with the tail gas flow rate in

Case II, 55,602 lb/hr. Furthermore, the flow rate of each tail gas component in Case I is almost identical with that in Case II except nitrogen flow rate, which is illustrated in Figure 14. In this regard, nitrogen flow rate is a dominant factor that differentiates each tail gas flow rate.

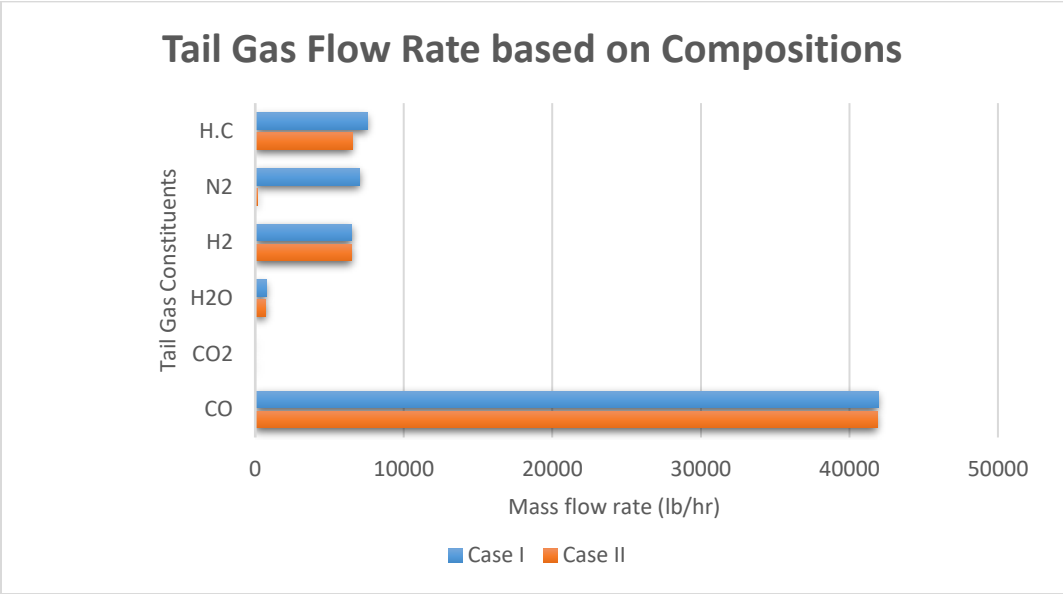

Figure 14 Tail gas flow rate based on compositions

6.2 F-T tail gas flow profile in accordance with tail gas fraction

While the F-T tail gas internal loop has advantage of generating power and reducing oxygen and steam consumption, it creates abnormal nitrogen flow simultaneously. The nitrogen flow is not enough to be neglected, which drives further investigation of tail gas utilization. Figure 15 presents the F-T tail gas flow profile according to F-T tail gas distribution.

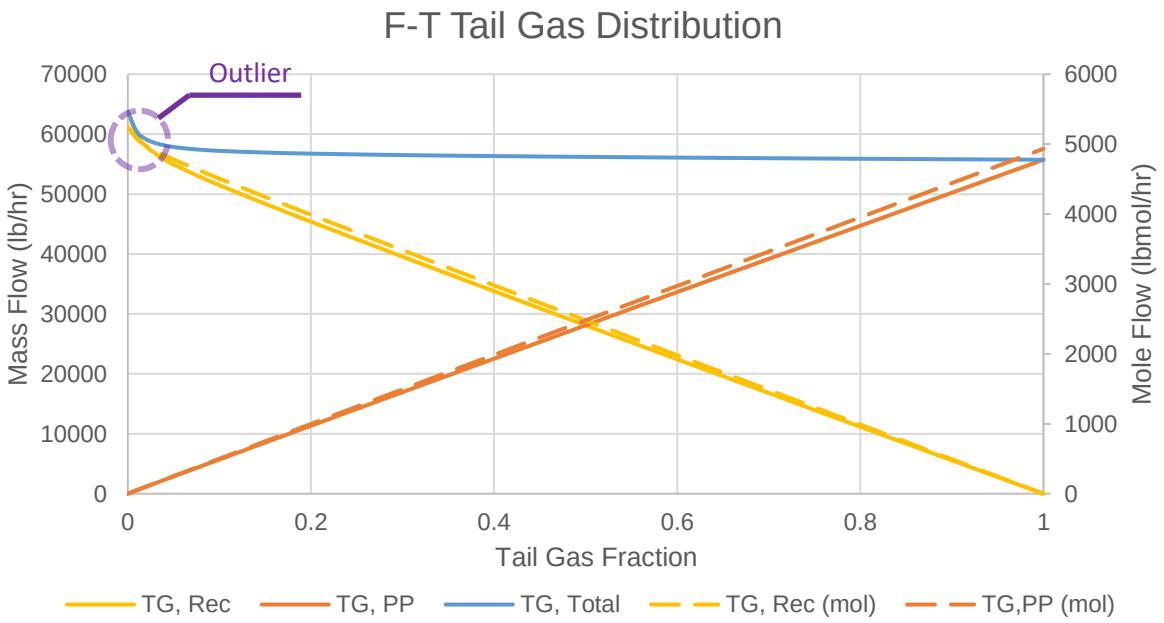

Figure 15 F-T tail gas flow profile

In Figure 15, The x-axis corresponds to tail gas fraction. It determines the split ratio of the F-T tail gas. The value, zero (0), indicates that all of the F-T tail gas is recycled to the GTL plant, whereas the value, one (1), shows that all of the F-T tail gas goes to the power plant. In case that the value is 0.5, tail gas is split evenly into each side. The F-T tail gas fed to the power plant is expressed by red line, while the recycled tail gas is represented by yellow line. The blue line indicates the sum of both F-T tail gases. The graph is straightforward except the region of extremely low tail gas fraction. The total F-T tail gas flow rate drastically increases on that region as the tail gas fraction decreases. This outlier is addressed by reviewing each component flow rate in accordance with the tail gas fraction.

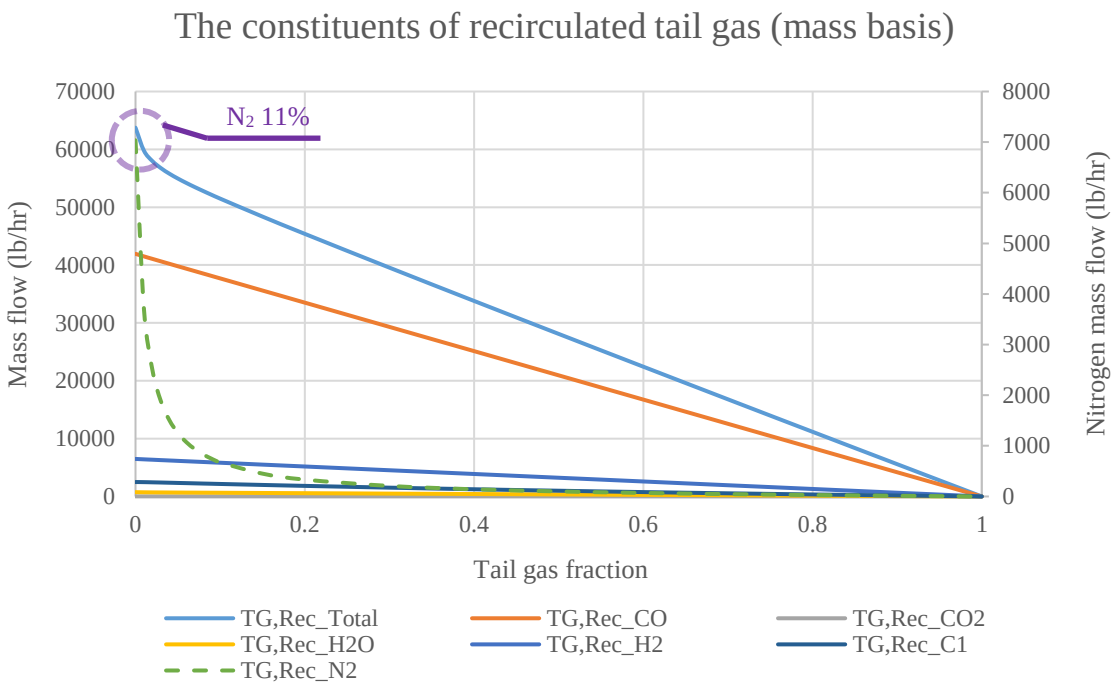

Figure 16 Tail gas constituents flow profile (mass basis)

Figure 16 shows the profile of each composition in mass flow basis. Most constituents increase as tail gas fraction decreases with different slopes. Among the constituents, nitrogen soars around zero (0) tail gas fraction. It results in the increase in the total F-T tail gas. Also, the graph for tail gas constituents in mole flow basis is consistent with that in mass flow basis. Figure 17 shows that nitrogen mole flow rate also rises steeply. The graphs in the Figure 16 and Figure 17 emphasizes the importance of nitrogen evacuation. It is noted that the nitrogen flow is abnormally high only in the range of low tail gas fraction values, which allows that even small increase in tail gas fraction can relieve unnecessary nitrogen accumulation in the GTL process.

Before limiting the tail gas fraction to avoid atypical nitrogen flow establishment, it is necessary to discuss the difference of nitrogen flow percentage between Figure 16 and Figure 17. Nitrogen flow accounts for 11% of total flow on the mass flow basis, while it is below 5% on the

mole flow basis. Between two properties, mole flow rather than mass flow governs equipment sizing in real projects because it is associated with volumetric flow. In this regard, it needs to review whether neglecting nitrogen mole flow in F-T tail gas is applicable.

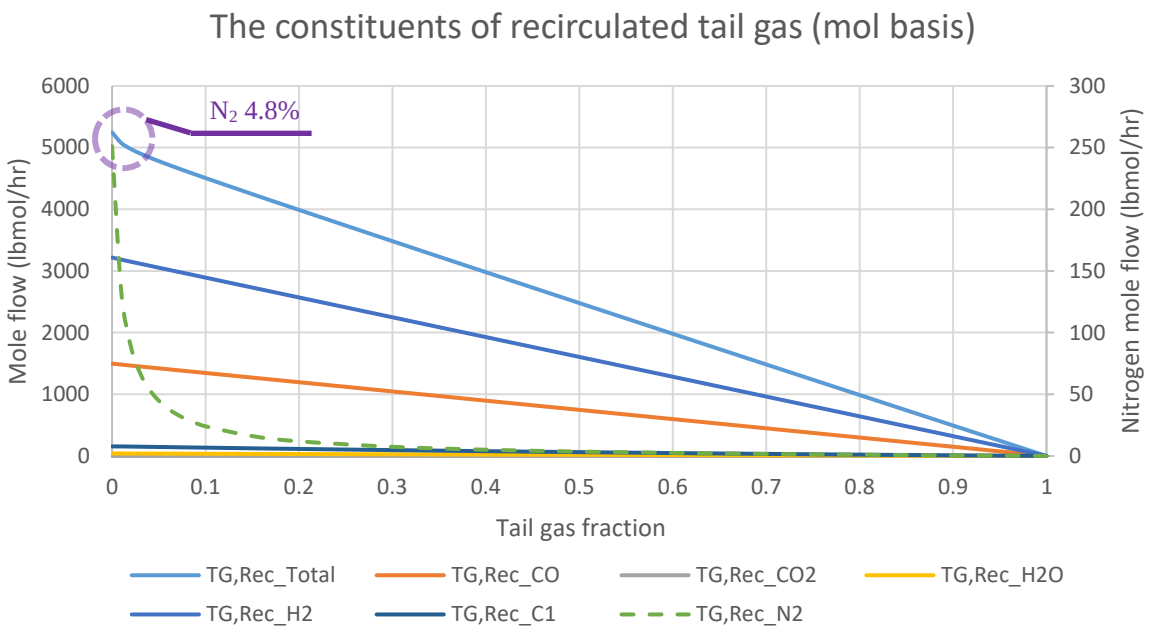

Figure 17 The graph for recirculated tail gas constituents flow (mol basis)

6.3 The review of nitrogen buildup in the F-T tail gas

The nitrogen in the F-T tail gas comes from natural gas only. Other sources such as steam, water and oxygen do not supply nitrogen to the GTL plant. Since natural gas is a nitrogen supplier, it is necessary to find out the relationship between natural gas and F-T tail gas in terms of nitrogen content.

Parameter	Value
The input value of nitrogen concentration in simulation [1, 45]	0.08 %
The limit of total inert gas in the U.S. National Pipeline [70]	Below 4 %

Table 8 The information of nitrogen concentration in natural gas

Table 8 presents the information on nitrogen concentration and its limitation in the U.S. national pipeline. This information implies two things: One is the variability of nitrogen concentration, and the other is that the nitrogen concentration in simulation, 0.08%, is too low to represent actual natural gas composition. As the way of supplementing former study results, the additional values of the nitrogen concentration are selected between 0% to nearly 1 %. In this range, the trend of nitrogen mole percentage in F-T tail gas is shown as Table 9.

N_2 in Natural Gas (% mol)	N_2 in Natural Gas (% mass)	N_2 in Tail Gas (% mol)	N_2 in Tail Gas (% mass)
0%	0%	0%	0%
0.08%	0.13%	4.8%	11.0%
0.14%	0.24%	8.3%	18.2%
0.29%	0.48%	15.3%	30.8%
0.43%	0.71%	21.5%	40.2%
0.57%	0.95%	26.8%	47.4%
0.71%	1.19%	31.5%	53.0%
0.85%	1.42%	35.7%	57.6%
0.99%	1.66%	39.4%	61.4%

Table 9 The relationship of nitrogen mole % in between the natural gas and the F-T tail gas

According to the former result in Figure 17, the nitrogen mole percentage in the F-T tail gas is 4.8 %. However, it reaches 39.4% in the case that the nitrogen content in the natural gas is about 1%. Moreover, it is expected that the higher the nitrogen concentration in the natural gas is, the higher the nitrogen mole percentage in the F-T tail gas is.

As the worst case described in Table 8, the nitrogen mole concentration is considered as 4% and other constituents are normalized. In this condition, the nitrogen constituent of the fluid upstream of F-T reactor is shown in Figure 18.

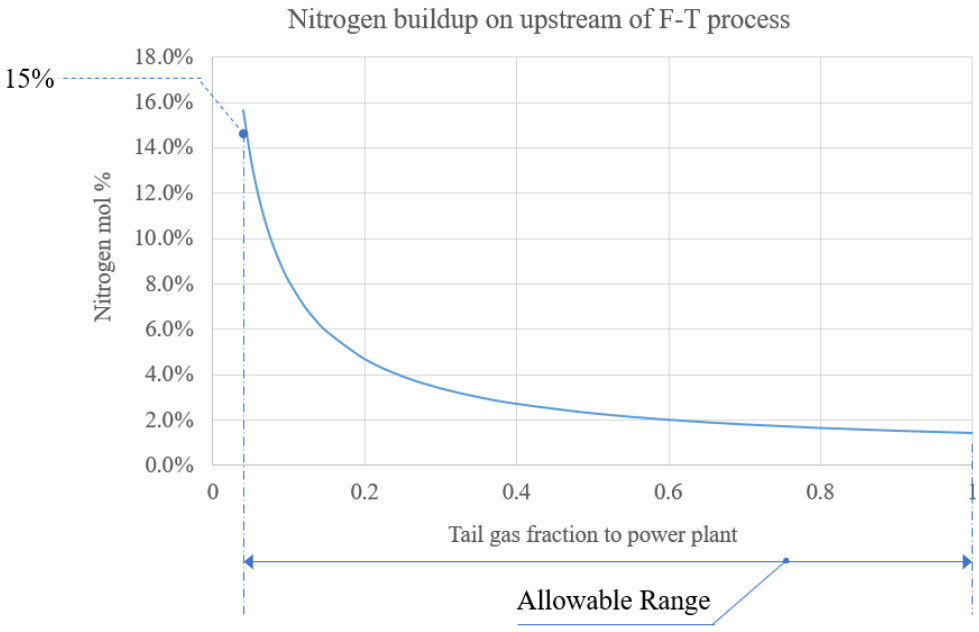

Figure 18 Nitrogen compound buildup on upstream F-T process flow

The nitrogen mole percentage rises considerably at low tail gas fraction, which is consistent with the graph in Figure 18. Based on the 'soft maximum' specification of nitrogen flow, 15 %, [30] around 0.05 or above for tail gas fraction is acceptable. Moreover, it is preferred to set the tail gas

fraction as high as possible.[30] Reducing the nitrogen mole percentage enables to downsize equipment in the GTL plant.

6.4 The evacuation route of nitrogen

In addition to the nitrogen concentration in natural gas, the GTL plant configuration is the other factor that increases nitrogen flow. Since nitrogen comes into the GTL plant with other natural gas compositions, a discharging route is required. Originally, the F-T tail gas path expressed as the dotted line in Figure 19 is a route through which inert gases go out of the GTL plant. However, it becomes a close loop when all tail gas is recycled. The loop cannot serve to evacuate nitrogen. Instead, the nitrogen is emitted to atmosphere through other routes illustrated in the Figure 19.

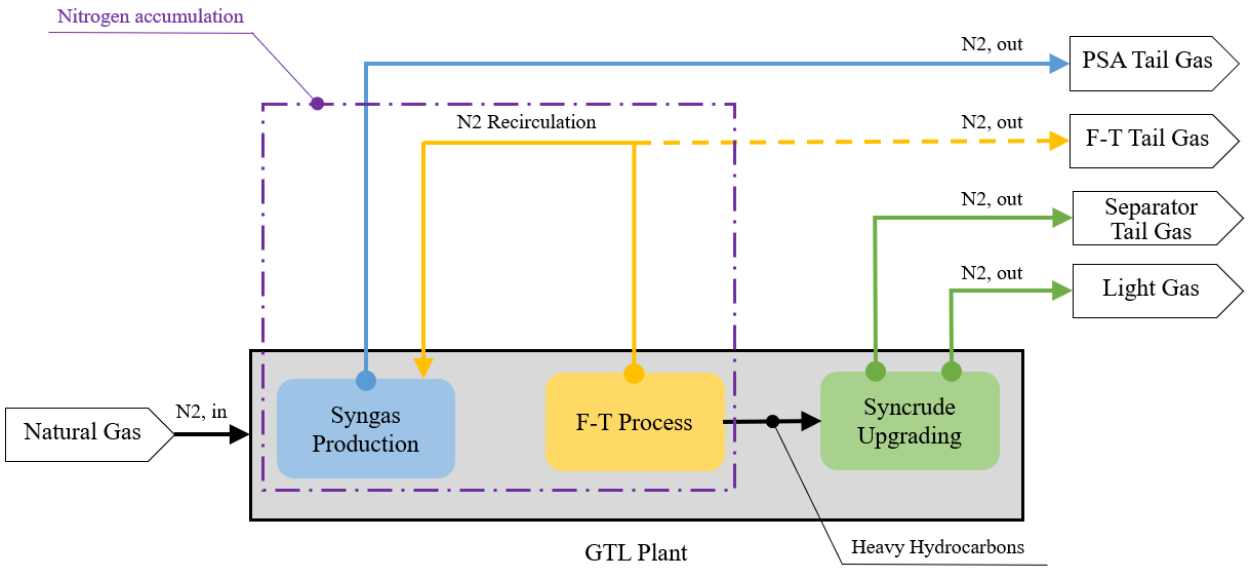

Figure 19 Nitrogen gas flow diagram

According to Figure 19, three (3) pathways still exist when F-T tail gas is fully recycled. However, two (2) lines from the syncrude upgrading process are not effective for the evacuation. The underlying reason is that heavier hydrocarbons are main constituents of the fluid transferred from the F-T process to the syncrude upgrading process. Instead of these lines, the discharge line for the PSA tail gas undertakes the role.

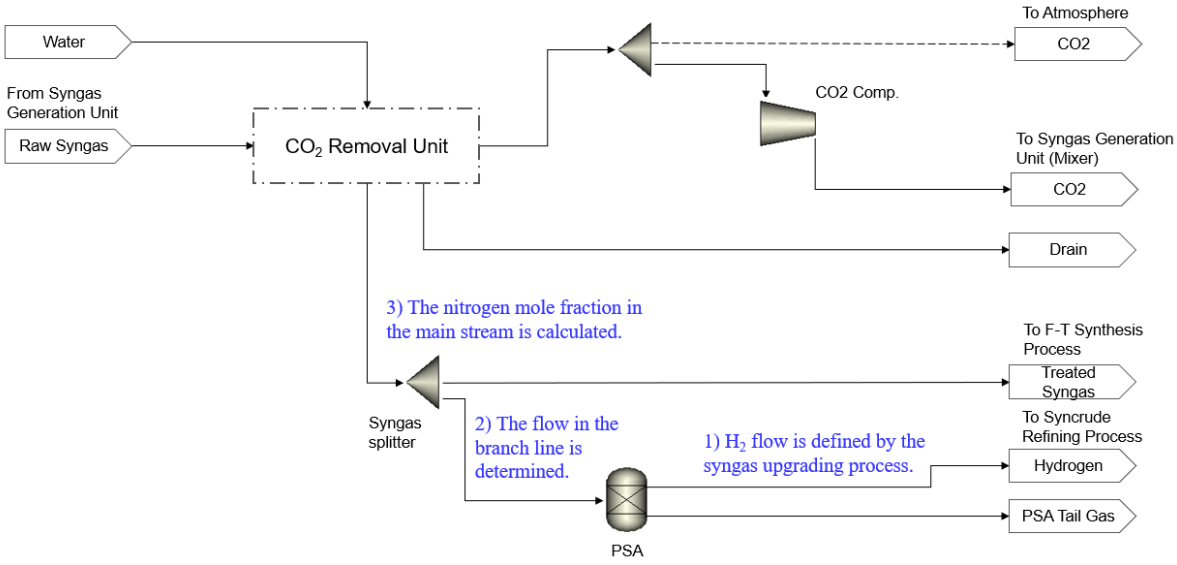

Figure 20 The steps to calculate nitrogen flow in main stream[1]

While the PSA tail gas line prevents the worst scenario that no route exists for evacuation, the issue is not resolved completely. It results in the accumulation of nitrogen concentration in the syngas production process and the F-T process. The three steps to calculate the nitrogen concentration are described in Figure 20. In the first step, hydrogen required by the syncrude upgrading process is defined. Then the hydrogen determines the flow in the branch line for the PSA unit. By using this flow, the nitrogen mole fraction in the main stream is calculated in the last

step. These steps imply the evacuation is executed indirectly. In other words, it is unavoidable to resolve this issue under the current configuration.

In summary, the role of the F-T tail gas route as evacuation is essential to stop increasing nitrogen gas flow. It is difficult to take over the role to other existing routes. At least, a part of the F-T tail gas should be evacuated from the GTL process in order to minimize the impact on equipment sizing. For process integration, this factor is one constraint that limits the adjustment of the tail gas fraction.

6.5 The review of power plant fuel compositions

In the GTL plant, the range of the tail gas fraction is restricted due to nitrogen buildup. Likewise, the power plant has the issue on fuel compositions that hinder process integration. The gas turbine, one of main equipment in the combined cycle power plant, requires to follow standards given by gas turbine manufacturers. Thus, it is necessary to analyze blended fuel compositions and confirm it complies with the requirement.

The power plant fuel is the mixture of the F-T tail gas and the natural gas. The power plant receives this mixture except the case that either F-T tail gas or the natural gas is supplied. Figure 21 and Figure 22 present the compositions of blended fuel.

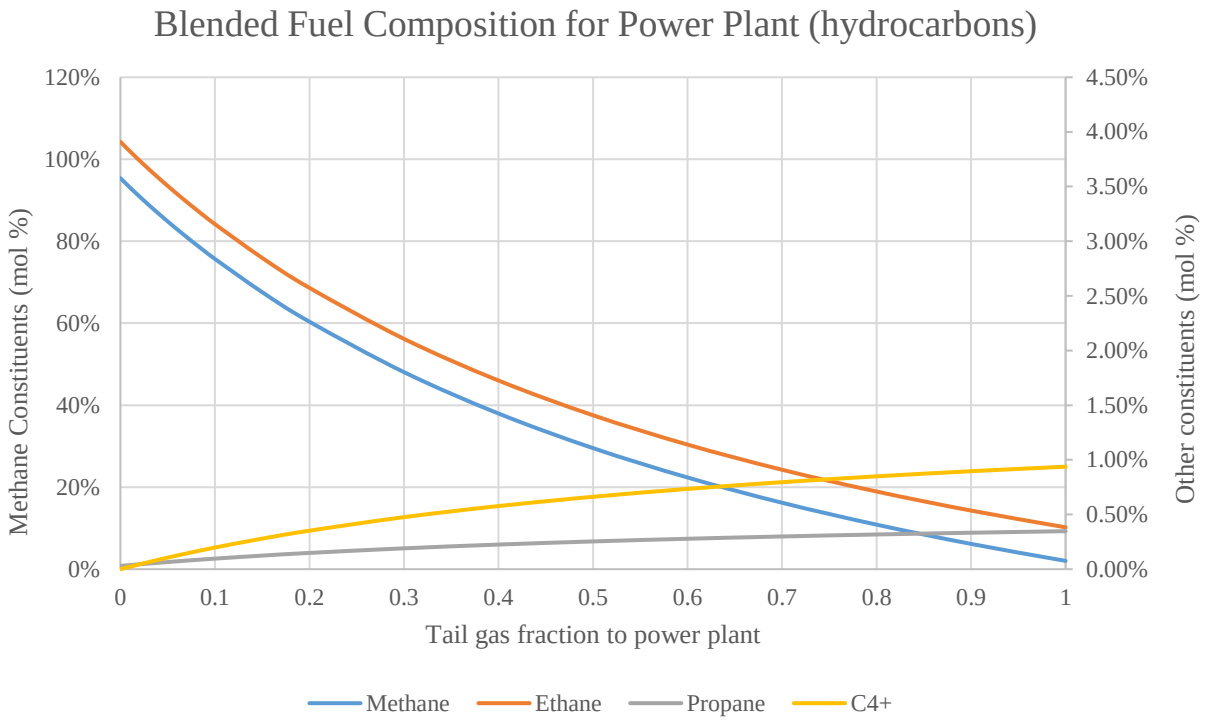

Figure 21 Blended fuel composition (hydrocarbons)

In Figure 21, methane mole fraction is the highest at zero (0) tail gas fraction whereas it is the lowest at one (1) tail gas fraction. It results from that the concentration of methane in the natural gas is much higher than that in the F-T tail gas. The reason that the graph for methane is not a straight line but a curve is that the slope of tail gas flow is steeper than that of natural gas, which is described in Figure 22. Likewise, the graph for ethane is not linear. Ethane also goes down as natural gas flow rate increases. On the other hand, propane and C_4^+ hydrocarbons have opposite trends, which are derived from the origin of the compositions. The propane is mostly from the F-T tail gas. All C_4^+ hydrocarbons are from the F-T tail gas.

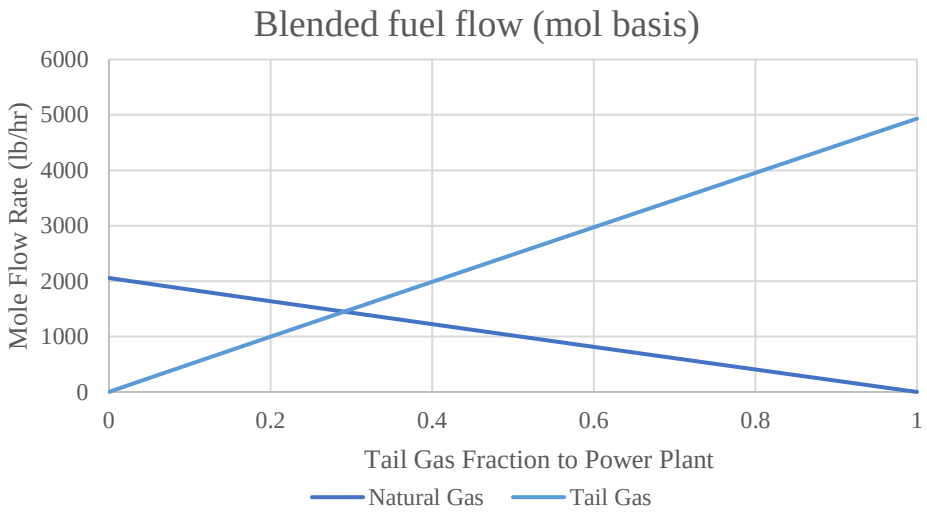

Figure 22 Blended fuel flow (mol basis)

According to Figure 23, the graphs of hydrogen and carbon monoxide are similar with those of propane and C_4^+ hydrocarbons. However, their variations are quite different. Even the hydrogen and carbon monoxide account for 95% of the tail gas flow when tail gas fraction is one.

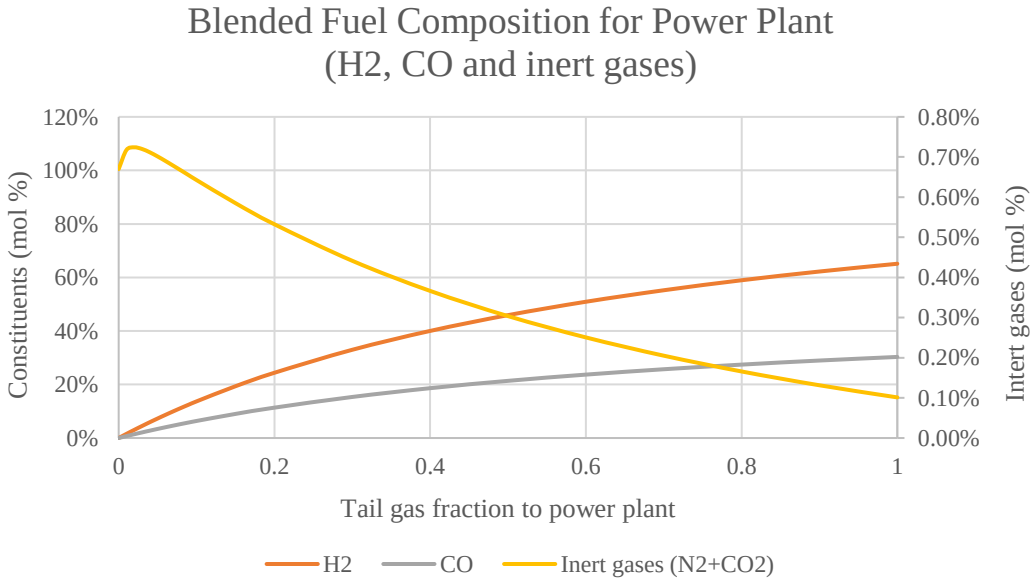

Figure 23 blended fuel composition (H_2, CO and inert gases)

When it comes to inert gases, it reaches the highest point when tail gas fraction is around 0.02, and it starts to decrease after the peak. When tail gas fraction is very low, the trend of this graph is due to the nitrogen flow rate in tail gas. In Figure 24, the inclination of nitrogen flow rate in tail gas is comparable to that of other compositions' flow rates. However, the inert gas mole fraction in blended gas at peak is small because it is mixed with large amount of natural gas. After the peak, the inert gases mole percentage decreases because the flows of other components in tail gas keep increasing. Moreover, the increase rate of nitrogen mole flow is lower than that of other components' mole flow. For these reasons, the nitrogen mole percentage on the blended gas is negligible throughout the range of the tail gas fraction. In addition to the nitrogen, carbon dioxide is small enough to be neglected.

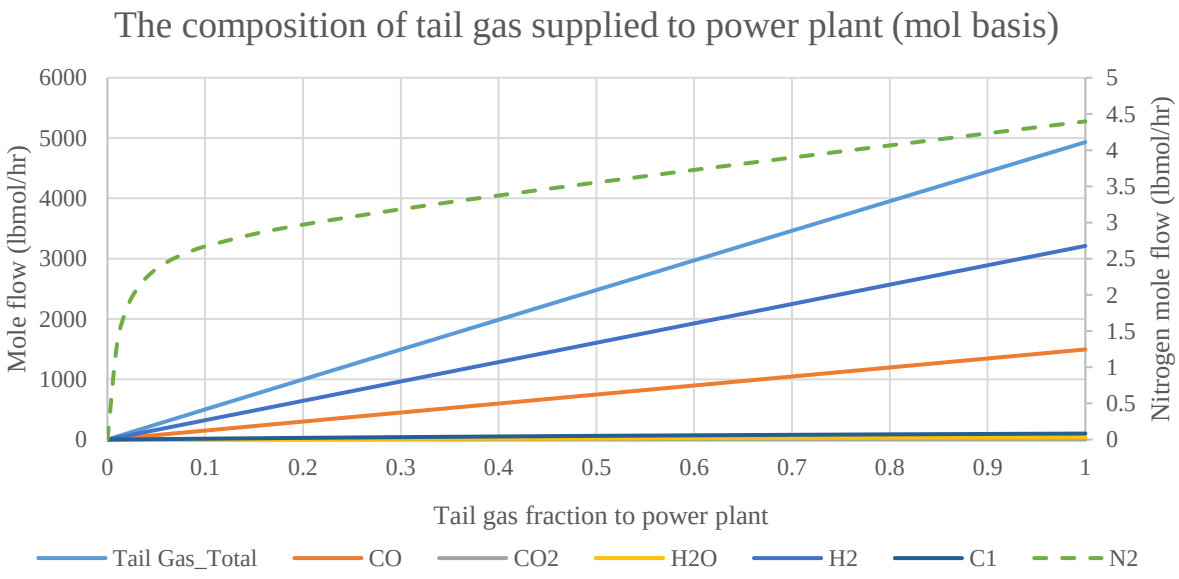

Figure 24 The composition of F-T tail gas supplied to power plant (mol basis)

6.6 Modified wobbe index variation from fuel blending

Modified wobbe index (MWI) is one of the most important parameters on a gas turbine. It should be within an allowable range for the gas turbine to accommodate fuel variation. The MWI formula is expressed as Equation 7).[40]

$$\text{MWI} = \frac{LHV}{\sqrt{T \times Specific\ Gravity}} = \frac{LHV}{\sqrt{T \times \frac{MW_{fuel}}{28.96}}} \quad \text{Equation 7)}$$

Equation 7) indicates that the MWI relies on three properties: fuel temperature, lower heating value (LHV) and molecular weight (MW). The fuel temperature is fixed in this study. On the contrary, both the MW and the LHV are calculated based on the property of each fuel composition, which is referred from ASTM D 3588. Blending the natural gas and the F-T tail gas leads to the change of both properties, which requires to confirm MWI values are within allowable MWI ranges of gas turbines. The allowable MWI ranges are specified in Table 10.[56, 71]

Gas turbine	7E.03	7F.04	7F.05, 7F.06	7HA.01, 7HA.02
MWI variation	±30%	+20%, -10% (5ppm NOx)	±7.5%	±10%

Table 10 The allowable MWI ranges

Among gas turbines specified in Table 10, the 7E.03 gas turbine has the widest MWI range. In other words, it is adequate to cover fuel variation compared to other gas turbines. For this reason, the 7E.03 gas turbine is selected for the following analysis.

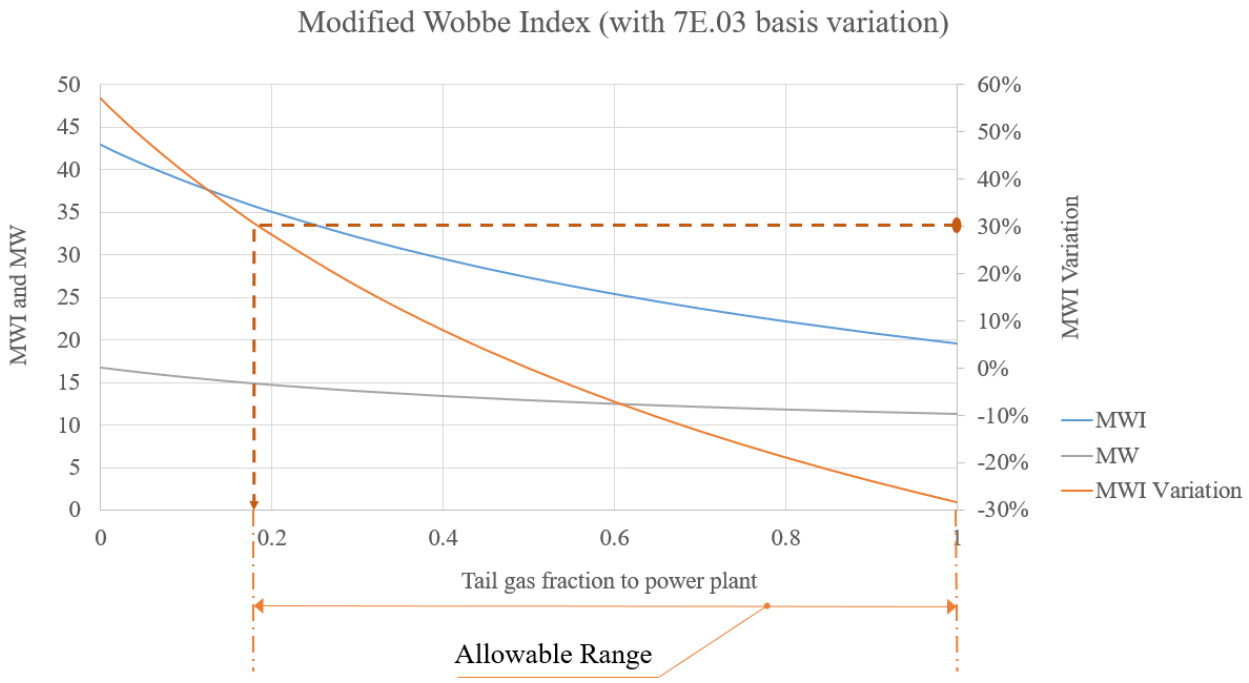

Figure 25 Modified wobbe index of blended fuel (with 7E.03 variation)

The plots for the MWI range is presented in Figure 25. When it comes to molecular weight, it goes down when the tail gas fraction increases. It is caused by the fact that the molecular weight of the F-T tail gas is lower than that of the natural gas. Modified wobbe index also decreases as tail gas fraction goes up despite the trend of the molecular weight. This result implies that the effect of the lower heating value is much more than that of the molecular weight for modified wobbe index calculation. From the graph of MWI variation, it is confirmed that the 7E.03 gas turbine allows the adjustment of the tail gas fraction from around 0.19 to 1.

6.7 The result of process integration with constraints

The two issues, nitrogen buildup and MWI limitation, create constraints that restrict process integration. With these constraints, the result of the process integration is illustrated in Figure 26.

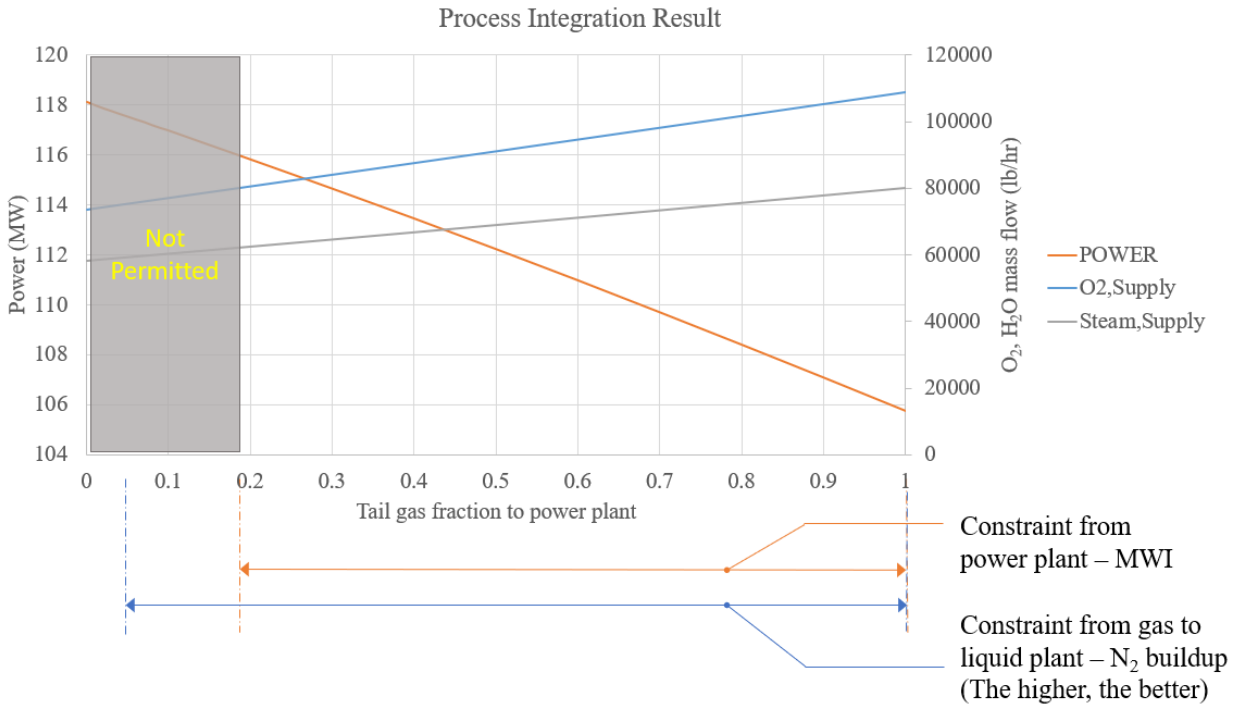

Figure 26 Process integration result with constraints

Originally, the F-T tail gas is freely distributed to two discrete plants by selecting any tail gas fraction value. However, the allowable range of F-T tail gas distribution is limited by the constraints derived from both the GTL plant and the power plant. Between two constraints, the constraint from the power plant regarding modified wobbe index range limit is stricter than the other constraint from the GTL plant. Thus, the MWI limit defines the allowable range of the tail gas fraction.

Within the allowable range, any value of the tail gas fraction can be selected. However, it There is a tradeoff among power output, utility consumption and nitrogen compound buildup, which is summarized in Table 11.

Tail gas fraction (to a power plant)	Low	High
Power output	↑	↓
Steam and oxygen consumption	↓	↑
Nitrogen compound buildup	↑	↓

Table 11 Trade-off among power output, utility consumption and nitrogen buildup

7. CONCLUSION AND DISCUSSION

Through this study, it is confirmed that process integration of a GTL plant and a power plant is feasible within the constraints. Despite the constraints from both plants, the integrated plant still has the allowable range to control F-T tail gas fraction. Since each tail gas fraction value has pros and cons in the perspective of power output, utility consumption and nitrogen buildup, it is necessary to analyze the effect of the adjustment to decide the extent of flexibility.

In addition to the result of the simulation, remaining issues are described as follows:

- The 7E.03 gas turbine is a suitable model for process integration because it has the widest range of MWI. However, its capacity is not sufficient to be integrated with a large-scale GTL plant. Improving fuel-flexibility on large capacity gas turbines is necessary.[72]
- In case of diffusion type combustors, they have several methods such as steam injection, nitrogen injection and SCR to reduce NOx emission.[73, 74] Since each method needs a relevant utility source, the utility consumption of a power plant should be considered. In case of NOx abatement with the nitrogen injection, the air separation unit of a GTL plant for pure oxygen generation can provide high concentration nitrogen gas to the power plant.
- In the simulation model, all off gases including PSA tail gas, separator tail gas and light gas are discharged to the atmosphere except F-T tail gas. The purpose of this setting is to focus on F-T tail gas utilization. However, it is not reasonable in terms of energy sustainability. The utilization of the off gases in a power plant can increase power output.
- F-T tail gas has heavy hydrocarbon contents. If they are not acceptable to a gas turbine, tail gas treatment system should be prepared.

- If nitrogen gas buildup in a GTL process reduces the partial pressure of syngas, reaction rate in F-T synthesis process can be affected negatively.[32] It can be one reason that the nitrogen gas buildup should be minimized. If the minimum allowable F-T tail gas fraction from a GTL plant is higher than that from a power plant, the allowable range for integrated plant operation will decrease.

REFERENCES

1. Gabriel, K. J.; Linke, P.; Jiménez-Gutiérrez, A.; Martínez, D. Y.; Noureldin, M.; El-Halwagi, M. M., Targeting of the water-energy nexus in gas-to-liquid processes: A comparison of syngas technologies. *Industrial & Engineering Chemistry Research* **2014,** *53* (17), 7087-7102.

2. Fleisch, T.; Sills, R.; Briscoe, M., A review of global GTL developments. *journal of natural gas chemistry* **2002,** *11*, 1-14.

3. Sieminski, A. In *International Energy Outlook. Energy Information Administration (EIA)*, 2014.

4. Shell SHELL WILL NOT PURSUE US GULF COAST GTL PROJECT. https://www.shell.com/media/news-and-media-releases/2013/shell-will-not-pursue-us-gulf-coast-gtl-project.html#vanity-aHR0cHM6Ly93d3cuc2hlbGwuY29tL2dsb2JhbC9hYm91dHNoZWxsL21lZGlhL25ld3MtYW5kLW1lZGlhLXJlbGVhc2VzLzIwMTMvc2hlbGwtd2lsbC1ub3QtcHVyc3VlLXVzLWd1bGYtY29hc3QtZ3RsLXByb2plY3QuaHRtbA (accessed January 16th, 2018).

5. Sasoal SASOL UNVEILS STRATEGY TO DRIVE FUTURE VALUE-BASED GROWTH. http://www.sasol.com/media-centre/media-releases/sasol-unveils-strategy-drive-future-value-based-growth (accessed January 16th, 2018).

6. Wood, D. A.; Nwaoha, C.; Towler, B. F., Gas-to-liquids (GTL): A review of an industry offering several routes for monetizing natural gas. *Journal of Natural Gas Science and Engineering* **2012,** *9*, 196-208.

7. Martínez, D. Y.; Jiménez-Gutiérrez, A.; Linke, P.; Gabriel, K. J.; Noureldin, M. M.; El-Halwagi, M. M., Water and energy issues in gas-to-liquid processes: assessment and integration

of different gas-reforming alternatives. *ACS Sustainable Chemistry & Engineering* **2013,** *2* (2), 216-225.

8. Wilhelm, D.; Simbeck, D.; Karp, A.; Dickenson, R., Syngas production for gas-to-liquids applications: technologies, issues and outlook. *Fuel processing technology* **2001,** *71* (1-3), 139-148.

9. Cho, W.; Song, T.; Mitsos, A.; McKinnon, J. T.; Ko, G. H.; Tolsma, J. E.; Denholm, D.; Park, T., Optimal design and operation of a natural gas tri-reforming reactor for DME synthesis. *Catalysis Today* **2009,** *139* (4), 261-267.

10. Majewski, A. J.; Wood, J., Tri-reforming of methane over Ni@ SiO2 catalyst. *International Journal of Hydrogen Energy* **2014,** *39* (24), 12578-12585.

11. Noureldin, M. M.; Elbashir, N. O.; El-Halwagi, M. M., Optimization and selection of reforming approaches for syngas generation from natural/shale gas. *Industrial & Engineering Chemistry Research* **2013,** *53* (5), 1841-1855.

12. Barbieri, G.; Violante, V.; Di Maio, F. P.; Criscuoli, A.; Drioli, E., Methane steam reforming analysis in a palladium-based catalytic membrane reactor. *Industrial & engineering chemistry research* **1997,** *36* (8), 3369-3374.

13. Sehested, J., Four challenges for nickel steam-reforming catalysts. *Catalysis Today* **2006,** *111* (1-2), 103-110.

14. Hickman, D.; Schmidt, L., Production of syngas by direct catalytic oxidation of methane. *science* **1993,** *259* (5093), 343-346.

15. Ghoneim, S. A.; El-Salamony, R. A.; El-Temtamy, S. A., Review on innovative catalytic reforming of natural gas to syngas. *World Journal of Engineering and Technology* **2015,** *4* (01), 116.

16. Bao, B.; El-Halwagi, M. M.; Elbashir, N. O., Simulation, integration, and economic analysis of gas-to-liquid processes. *Fuel Processing Technology* **2010,** *91* (7), 703-713.

17. Bharadwaj, S.; Schmidt, L., Catalytic partial oxidation of natural gas to syngas. *Fuel processing technology* **1995,** *42* (2-3), 109-127.

18. Al-Douri, A.; Sengupta, D.; El-Halwagi, M. M., Shale gas monetization–A review of downstream processing to chemicals and fuels. *Journal of Natural Gas Science and Engineering* **2017,** *45*, 436-455.

19. Vosloo, A. C., Fischer–Tropsch: a futuristic view. *Fuel processing technology* **2001,** *71* (1-3), 149-155.

20. Moodley, D.; Van De Loosdrecht, J.; Saib, A.; Niemantsverdriet, H., The formation and influence of carbon on cobalt-based Fischer-Tropsch synthesis catalysts. *Advances in Fischer-Tropsch synthesis, catalysts, and catalysis* **2010**.

21. Ross, J.; Van Keulen, A.; Hegarty, M.; Seshan, K., The catalytic conversion of natural gas to useful products. *Catalysis Today* **1996,** *30* (1-3), 193-199.

22. Raju, A. S.; Park, C. S.; Norbeck, J. M., Synthesis gas production using steam hydrogasification and steam reforming. *Fuel Processing Technology* **2009,** *90* (2), 330-336.

23. Minutillo, M.; Perna, A., A novel approach for treatment of CO2 from fossil fired power plants. Part B: The energy suitability of integrated tri-reforming power plants (ITRPPs) for methanol production. *international journal of hydrogen energy* **2010,** *35* (13), 7012-7020.

24. Murmura, M.; Diana, M.; Spera, R.; Annesini, M., Modeling of autothermal methane steam reforming: Comparison of reactor configurations. *Chemical Engineering and Processing: Process Intensification* **2016,** *109*, 125-135.

25. Dry, M. E., The fischer–tropsch process: 1950–2000. *Catalysis today* **2002,** *71* (3-4), 227-241.

26. Riedel, T.; Claeys, M.; Schulz, H.; Schaub, G.; Nam, S.-S.; Jun, K.-W.; Choi, M.-J.; Kishan, G.; Lee, K.-W., Comparative study of Fischer–Tropsch synthesis with H2/CO and H2/CO2 syngas using Fe-and Co-based catalysts. *Applied Catalysis A: General* **1999,** *186* (1-2), 201-213.

27. Kim, S.-M.; Bae, J. W.; Lee, Y.-J.; Jun, K.-W., Effect of CO2 in the feed stream on the deactivation of Co/γ-Al2O3 Fischer–Tropsch catalyst. *Catalysis Communications* **2008,** *9* (13), 2269-2273.

28. Patzlaff, J.; Liu, Y.; Graffmann, C.; Gaube, J., Studies on product distributions of iron and cobalt catalyzed Fischer–Tropsch synthesis. *Applied Catalysis A: General* **1999,** *186* (1-2), 109-119.

29. De Klerk, A., *Fischer-tropsch refining*. John Wiley & Sons: 2012.

30. Boerrigter, H.; Calis, H. P.; Slort, D. J.; Bodenstaff, H., Gas cleaning for integrated biomass gasification (BG) and Fischer-Tropsch (FT) systems; experimental demonstration of two BG-FT systems. *Acknowledgement/Preface* **2004,** *51*.

31. Lu, Y.; Lee, T., Influence of the feed gas composition on the Fischer-Tropsch synthesis in commercial operations. *Journal of Natural Gas Chemistry* **2007,** *16* (4), 329-341.

32. Kuntze, T. In *From natural gas to liquid hydrocarbons. Part 3. Kinetics of the Fischer-Tropsch synthesis using a nitrogen-rich synthesis gas*, Fuel and Energy Abstracts, 1995; p 416.

33. Jess, A.; Hedden, K.; Popp, R., Diesel Oil from Natural Gas by Fischer-Tropsch Synthesis Using Nitrogen-Rich Syngas. *Chemical Engineering & Technology: Industrial Chemistry-Plant Equipment-Process Engineering-Biotechnology* **2001,** *24* (1), 27-31.

34. Jess, A.; Popp, R.; Hedden, K., Fischer–Tropsch-synthesis with nitrogen-rich syngas: fundamentals and reactor design aspects. *Applied Catalysis A: General* **1999,** *186* (1-2), 321-342.

35. Baumgärtner, M.; Sattelmayer, T., Improvement of the turn-down ratio of gas turbines by autothermal on board syngas generation. *Journal of the Global Power and Propulsion Society* **2017,** *1*, D0HPA5.

36. Chacartegui, R.; Sánchez, D.; de Escalona, J. M.; Muñoz, A.; Sánchez, T., Gas and steam combined cycles for low calorific syngas fuels utilisation. *Applied energy* **2013,** *101*, 81-92.

37. Asai, T.; Miura, K.; Akiyama, Y.; Karishuku, M.; Yunoki, K.; Dodo, S.; Horii, N. In *Development Of Fuel-Flexible Gas Turbine Combustor*, Proceedings of the 45th Turbomachinery Symposium, Turbomachinery Laboratories, Texas A&M Engineering Experiment Station: 2016.

38. Chacartegui, R.; Sánchez, D.; de Escalona, J. M.; Jimenez-Espadafor, F.; Munoz, A.; Sánchez, T., SPHERA project: Assessing the use of syngas fuels in gas turbines and combined cycles from a global perspective. *Fuel processing technology* **2012,** *103*, 134-145.

39. Wright, I. G.; Gibbons, T., Recent developments in gas turbine materials and technology and their implications for syngas firing. *International Journal of Hydrogen Energy* **2007,** *32* (16), 3610-3621.

40. Campbell, A.; Goldmeer, J.; Healy, T.; Washam, R.; Molière, M.; Citeno, J. In *Heavy duty gas turbines fuel flexibility*, ASME Turbo Expo 2008: Power for Land, Sea, and Air, American Society of Mechanical Engineers: 2008; pp 1077-1085.

41. Payrhuber, K.; Jones, R. M.; Scholz, M. H. In *Gas turbine flexibility with carbon constrained fuels*, ASME Turbo Expo 2008: Power for Land, Sea, and Air, American Society of Mechanical Engineers: 2008; pp 937-943.

42. Brdar, R. D.; Jones, R. M., GE IGCC technology and experience with advanced gas turbines. *GE Power Systems, Schenectady, NY, Paper No. GER-4207* **2000**.

43. Gadde, S.; Wu, J.; Gulati, A.; McQuiggan, G.; Koestlin, B.; Prade, B. In *Syngas capable combustion systems development for advanced gas turbines*, ASME Turbo Expo 2006: Power for Land, Sea, and Air, American Society of Mechanical Engineers: 2006; pp 547-554.

44. Kehlhofer, R.; Hannemann, F.; Rukes, B.; Stirnimann, F., *Combined-cycle gas & steam turbine power plants*. Pennwell Books: 2009.

45. Srivatsan, J. S.; Amani, M., Feasibility study of using excess heat from GTL process for seawater desalination. *Energy and Environment Research* **2012,** *2* (1), 182.

46. Gas-To-Liquid (GTL) Technology Assessment in support of AEO2013. https://www.eia.gov/outlooks/documentation/workshops/pdf/AEO2013_GTL_Assessment.pdf (accessed June 1st, 2018).

47. Aasberg-Petersen, K.; Nielsen, C. S.; Dybkjær, I.; Perregaard, J., Large scale methanol production from natural gas. *Haldor Topsoe* **2008,** *22*.

48. Aasberg-Petersen, K.; Dybkjær, I.; Ovesen, C.; Schjødt, N.; Sehested, J.; Thomsen, S., Natural gas to synthesis gas–catalysts and catalytic processes. *Journal of Natural gas science and engineering* **2011,** *3* (2), 423-459.

49. Tristantini, D.; Lögdberg, S.; Gevert, B.; Borg, Ø.; Holmen, A., The effect of synthesis gas composition on the Fischer–Tropsch synthesis over Co/γ-Al2O3 and Co–Re/γ-Al2O3 catalysts. *Fuel processing technology* **2007,** *88* (7), 643-649.

50. Tsakoumis, N. E.; Voronov, A.; Rønning, M.; van Beek, W.; Borg, Ø.; Rytter, E.; Holmen, A., Fischer–Tropsch synthesis: An XAS/XRPD combined in situ study from catalyst activation to deactivation. *Journal of catalysis* **2012,** *291*, 138-148.

51. Dry, M. E., High quality diesel via the Fischer–Tropsch process–a review. *Journal of Chemical Technology and Biotechnology* **2002,** *77* (1), 43-50.

52. Kim, Y. H.; Jun, K.-W.; Joo, H.; Han, C.; Song, I. K., A simulation study on gas-to-liquid (natural gas to Fischer–Tropsch synthetic fuel) process optimization. *Chemical Engineering Journal* **2009,** *155* (1-2), 427-432.

53. Gabriel, K. J.; Noureldin, M.; El-Halwagi, M. M.; Linke, P.; Jiménez-Gutiérrez, A.; Martínez, D. Y., Gas-to-liquid (GTL) technology: Targets for process design and water-energy nexus. *Current Opinion in Chemical Engineering* **2014,** *5*, 49-54.

54. de Klerk, A., Fischer–Tropsch refining: technology selection to match molecules. *Green Chemistry* **2008,** *10* (12), 1249-1279.

55. Dancuart, L.; De Haan, R.; De Klerk, A., Processing of primary Fischer-Tropsch products. In *Studies in Surface Science and Catalysis*, Elsevier: 2004; Vol. 152, pp 482-532.

56. GEA32932 7E Power Plants - GE.com. https://www.ge.com/content/dam/gepower-pgdp/global/en_US/documents/product/gas%20turbines/Fact%20Sheet/2018-prod-specs/7E-power-plants.pdf (accessed June 1st, 2018).

57. Jonsson, M.; Bolland, O.; Bücker, D.; Rost, M., Gas turbine cooling model for evaluation of novel cycles. *Proceedings of ECOS* **2005**, 20-22.

58. Kim, T.; Ro, S., Power augmentation of combined cycle power plants using cold energy of liquefied natural gas. *Energy* **2000,** *25* (9), 841-856.

59. Thattai, A. T.; Wittebrood, B.; Woudstra, T.; Geerlings, J.; Aravind, P., Thermodynamic system studies for a natural gas combined cycle (NGCC) plant with CO2 capture and hydrogen storage with metal hydrides. *Energy Procedia* **2014,** *63*, 1996-2007.

60. Kim, T., Comparative analysis on the part load performance of combined cycle plants considering design performance and power control strategy. *Energy* **2004,** *29* (1), 71-85.

61. Casarosa, C.; Donatini, F.; Franco, A., Thermoeconomic optimization of heat recovery steam generators operating parameters for combined plants. *Energy* **2004,** *29* (3), 389-414.

62. Arrieta, F. R. P.; Lora, E. E. S., Influence of ambient temperature on combined-cycle power-plant performance. *Applied Energy* **2005,** *80* (3), 261-272.

63. Ion, D.; Codrut, P., Efficiency Assessment of Condensing Steam Turbine. *Advances in Environment, Ecosystems and Sustainable Tourism* **2013**, 203e208.

64. Christian M. Gomes, W. L. R. G. In *Modeling part-load performance of a gas turbine*, Proceedings of COBEM 2003, Sao Paulo, SP, Sao Paulo, SP, 2003.

65. Johnson, M. S., Prediction of gas turbine on-and off-design performance when firing coal-derived syngas. *Journal of engineering for gas turbines and power* **1992,** *114* (2), 380-385.

66. Razak, A., *Industrial gas turbines: performance and operability*. Elsevier: 2007.

67. Sánchez, D.; Chacartegui, R.; Munoz, J.; Muñoz, A.; Sanchez, T., Performance analysis of a heavy duty combined cycle power plant burning various syngas fuels. *international journal of hydrogen energy* **2010,** *35* (1), 337-345.

68. Oluyede, E. O.; Phillips, J. N. In *Fundamental impact of firing syngas in gas turbines*, ASME Turbo Expo 2007: Power for Land, Sea, and Air, American Society of Mechanical Engineers: 2007; pp 175-182.

69. He, F.; Li, Z.; Liu, P.; Ma, L.; Pistikopoulos, E. N., Operation window and part-load performance study of a syngas fired gas turbine. *Applied energy* **2012,** *89* (1), 133-141.

70. Foss, M. M.; Head, C., Interstate Natural Gas--Quality Specifications & Interchangeability. *Center for Energy Economics, Bureau of Economic Geology, University of Texas at Austin* **2004**.

71. GE Power 2016 Product catalog. https://powergen.gepower.com/content/dam/gepowerpgdp/global/en_US/documents/product/2016-gas-powersystems-products-catalog.pdf (accessed June 1st, 2018).

72. Jones, R.; Goldmeer, J.; Monetti, B., Addressing gas turbine fuel flexibility. *GE Energy Report GER4601 rev. B, October* **2011,** *29*, 2012.

73. Forzatti, P., Present status and perspectives in de-NOx SCR catalysis. *Applied catalysis A: general* **2001,** *222* (1-2), 221-236.

74. Chiesa, P.; Lozza, G.; Mazzocchi, L. In *Using hydrogen as gas turbine fuel*, ASME Turbo Expo 2003, collocated with the 2003 International Joint Power Generation Conference, American Society of Mechanical Engineers: 2003; pp 163-171.